Development/Plasticity/Repair

A Unilateral Negative Feedback Loop Between *miR-200* microRNAs and Sox2/E2F3 Controls Neural Progenitor Cell-Cycle Exit and Differentiation

Changgeng Peng,[1] Na Li,[2] Yen-Kar Ng,[1] Jingzhong Zhang,[1] Florian Meier,[1] Fabian J. Theis,[3] Matthias Merkenschlager,[4] Wei Chen,[2] Wolfgang Wurst,[1,5,6] and Nilima Prakash[1]

[1]Institute of Developmental Genetics, Helmholtz Zentrum München, Deutsches Forschungszentrum für Umwelt und Gesundheit, and Technische Universität München–Weihenstephan, D-85764 Neuherberg, Germany, [2]Berlin Institute for Medical Systems Biology, Max Delbrück Center for Molecular Medicine, D-13092 Berlin-Buch, Germany, [3]Computational Modeling in Biology, Institute of Bioinformatics and Systems Biology, Helmholtz Zentrum München, Deutsches Forschungszentrum für Umwelt und Gesundheit D-85764 Neuherberg, Germany, [4]Lymphocyte Development Group, Medical Research Council Clinical Sciences Centre, Imperial College, London W12 0NN, United Kingdom, [5]DZNE, Deutsches Zentrum für Neurodegenerative Erkrankungen Site Munich, D-80336 Munich, and [6]Max Planck Institute of Psychiatry, D-80804 Munich, Germany

MicroRNAs have emerged as key posttranscriptional regulators of gene expression during vertebrate development. We show that the *miR-200* family plays a crucial role for the proper generation and survival of ventral neuronal populations in the murine midbrain/hindbrain region, including midbrain dopaminergic neurons, by directly targeting the pluripotency factor Sox2 and the cell-cycle regulator E2F3 in neural stem/progenitor cells. The lack of a negative regulation of Sox2 and E2F3 by *miR-200* in conditional *Dicer1* mutants (*En1*$^{+/Cre}$; *Dicer1*$^{flox/flox}$ mice) and after *miR-200* knockdown *in vitro* leads to a strongly reduced cell-cycle exit and neuronal differentiation of ventral midbrain/hindbrain (vMH) neural progenitors, whereas the opposite effect is seen after *miR-200* overexpression in primary vMH cells. Expression of *miR-200* is in turn directly regulated by Sox2 and E2F3, thereby establishing a unilateral negative feedback loop required for the cell-cycle exit and neuronal differentiation of neural stem/progenitor cells. Our findings suggest that the posttranscriptional regulation of Sox2 and E2F3 by *miR-200* family members might be a general mechanism to control the transition from a pluripotent/multipotent stem/progenitor cell to a postmitotic and more differentiated cell.

Introduction

The mammalian midbrain/hindbrain region (MHR) harbors several neuronal populations with pivotal functions in normal brain physiology and behavior (Zervas et al., 2005). The development of this region relies on a tight control of gene regulatory networks active in the isthmic organizer (IsO), located at the midbrain/hindbrain boundary (MHB), and in the dorsal [roof plate (RP)] and ventral [floor plate (FP)] midline of the neural tube, including post-transcriptional or post-translational regulatory mechanisms (Wittmann et al., 2009).

MicroRNAs (miRNAs), a large class of small noncoding RNAs, have emerged as key posttranscriptional regulators of gene expression by targeting specific mRNAs for translational inhibition and degradation (Huntzinger and Izaurralde, 2011). During canonical miRNA biogenesis, miRNAs are transcribed by RNA polymerase II from their own promoter, rendering a larger and in many cases polycistronic primary transcript that is cleaved in the nucleus by a microprocessor complex into an ~70-nt-long precursor hairpin (pre-miRNA) and subsequently exported into the cytoplasm, in which it is cleaved by Dicer1 (an RNase III enzyme) into the mature ~22 nt miRNA duplex (Krol et al., 2010). One of the miRNA duplex strands is then assembled into the miRNA-induced silencing complex in which it acts as a guide strand for imperfect base pairing with its target mRNAs, encompassing up to several hundred mRNAs for each miRNA (Huntzinger and Izaurralde, 2011). A ~7-nt-long "seed" sequence within the 5′ terminus of the miRNA is most critical for target recognition in the 3′ untranslated region (UTR), 5′UTR, or coding sequence (CDS) of the mRNA (Mallanna and Rizzino, 2010).

Received May 2, 2012; revised July 25, 2012; accepted July 26, 2012.

Author contributions: C.P. and N.P. designed research; C.P., N.L., and Y.-K.N. performed research; J.Z., F.M., and M.M. contributed unpublished reagents/analytic tools; C.P., F.J.T., W.C., W.W., and N.P. analyzed data; C.P. and N.P. wrote the paper.

This work was supported by Bavarian Research Alliance "ForNeuroCell II" Grant F2-F2412.18/10 086 (W.W., N.P.), Federal Ministry of Education and Research Joint Project "Neurogenesis from Brain and Skin Cells" Grant FKZ 01GN1009C (W.W., N.P.), the Initiative and Networking Fund in the framework of the Helmholtz Alliances of Systems Biology and of Mental Health in an Ageing Society Grant HA-215 (W.W.), Federal Ministry of Education and Research National Genome Research Network Plus Project "From Disease Genes to Protein Pathways" Grant FKZ 01GS0858 (W.W.), and European Union Seventh Framework Programme Research Network SyBoSS Grant FP7-Health-F4-2010-242129 (W.W.). We thank D. Refojo and S. Giusti for the very generous gift of the pCAG–EGFP vector, G. Luxenhofer and A. Huber-Brösamle for the kind gift of pcDNA6.2–EmGFP plasmid, A. Kurz-Drexler for the pLL3.7 vector, and S. Laass for excellent technical assistance.

The authors declare no competing financial interests.

Correspondence should be addressed to either Nilima Prakash or Wolfgang Wurst, Institute of Developmental Genetics, Helmholtz Zentrum München, Deutsches Forschungszentrum für Umwelt und Gesundheit, and Technische Universität München-Weihenstephan, Ingolstädter Landstrasse 1, D-85764 Neuherberg, Germany. E-mail: nilima.prakash@helmholtz-muenchen.de.

DOI:10.1523/JNEUROSCI.2124-12.2012

 0270-6474/12/3213292-17$15.00/0

miRNAs are implicated in the regulation of numerous developmental processes, including the maintenance of self-renewing and pluripotent/multipotent embryonic stem cells (ESCs) and/or progenitor cells, and the differentiation of these pluripotent/multipotent cells into fate-committed cells (Pauli et al., 2011). According to their function and their targets in this context, miRNAs have been classified into either "ESC-specific cell-cycle-regulating (ESCC)" miRNAs, targeting negative regulators of cell-cycle progression, such as the retinoblastoma proteins, or "tissue-specific" miRNAs targeting (among others) the pluripotency transcription factors (TFs) Sox2, Oct4, Nanog, and c-Myc and the RNA-binding protein Lin28 (Ivey and Srivastava, 2010; Mallanna and Rizzino, 2010; Martinez and Gregory, 2010).

Based on the analysis of conditional mouse mutants for *Dicer1* in the MHR, we uncovered a novel function of *miR-200* in the CNS by showing that *miR-200* suppresses the expression of Sox2, a TF expressed in neural stem/progenitor cells and crucial for the maintenance of their proliferative capacity and multipotency (Pevny and Nicolis, 2010), and E2F3, a cyclic active TF required for the regulation of cell proliferation, differentiation, and survival (DeGregori, 2002), in neural progenitors. We also show that Sox2 and E2F3 in turn activate the transcription of *miR-200*, thereby establishing a unilateral negative feedback loop between the *miR-200* family and their targets Sox2 and E2F3 that regulates the cell-cycle exit and neuronal differentiation of neural stem/progenitor cells in the murine MHR but most likely also in other regions of the mammalian brain.

Materials and Methods

Mutant mice. *Dicer1*$^{flox/flox}$ female mice (Cobb et al., 2005) were crossed with male *En1*$^{+/Cre}$ mice (Kimmel et al., 2000) to obtain *En1*$^{+/Cre}$; *Dicer1*$^{+/flox}$ mice. Male *En1*$^{+/Cre}$; *Dicer1*$^{+/flox}$ mice were mated to female *Dicer1*$^{flox/flox}$ mice to obtain *En1*$^{+/Cre}$; *Dicer1*$^{flox/flox}$ embryos and pups. *En1*$^{+/Cre}$; *Dicer1*$^{+/flox}$, *En1*$^{+/+}$; *Dicer1*$^{+/flox}$, and *En1*$^{+/+}$; *Dicer1*$^{flox/flox}$ mice were used as wild-type controls. Fate-mapping of *Dicer1* mutant cells was done by crossing *En1*$^{+/Cre}$; *Dicer1*$^{+/flox}$ mice with *CAG–CAT–EGFP* transgenic mice (Nakamura et al., 2006). All mouse lines were kept in a mixed genetic background. C57BL/6 mice were purchased from Charles River. Timed pregnant females were used for collection of embryonic stages; noon of the day of vaginal plug detection was designated as embryonic day 0.5 (E0.5). Animal treatment was conducted under federal guidelines as approved by the Helmholtz Centre Munich Institutional Animal Care and Use Committee.

In situ *hybridization and histology.* Paraffin sections (8 μm) were processed for radioactive ([α-^{35}S]UTP; GE Healthcare) *in situ* hybridization (ISH) as described previously (Fischer et al., 2007). Riboprobes used were *Dicer1* [complementary to exons 21–22 that are deleted in *Dicer1* conditional knock-out (*cKO*) mice], *En1*, *Wnt1*, *Fgf8*, *Lmxb1*, *Otx2*, *Gbx2*, *Shh*, *Pax2*, *Sef* (*Il17rd*), *Spry1*, *Spry2*, *Dusp6* (*Mkp3*), *Hes1*, *Hes3*, and *Hes5* (Puelles et al., 2004; Fischer et al., 2007, 2011). Details on riboprobes are available on request. Locked nucleic acid (LNA) oligonucleotide-based ISH using unlabeled LNA-modified *mmu-miR-124* (EQ 56993; Exiqon), *mmu-miR-200c* (EQ 56944; Exiqon), and scramble-miR control (catalog #99004-00; Exiqon) detection probes was performed on 8 μm paraffin sections as described previously (Silahtaroglu et al., 2007). The LNA-modified detection probes were labeled with [^{35}S]dATP (GE Healthcare) or digoxigenin (DIG)–dUTP using the DIG Oligonucleotide Tailing Kit or DIG Oligonucleotide 3′-End Labeling Kit (Roche) according to the instructions of the manufacturer. Sections were counterstained with cresyl violet (0.5%; Sigma) following standard procedures. Images were taken using bright- and dark-field optics on an Axioplan2 microscope or StemiSV6 stereomicroscope, AxioCam MRc camera, and Axiovision 4.6 software (Carl Zeiss) and processed with Adobe Photoshop CS software (Adobe Systems).

Immunostainings. Immunostainings on 8 μm paraffin sections and cultured cells were performed as described previously (Peng et al., 2011). Polyclonal rabbit antisera were directed against cleaved (activated) Caspase-3 (cCaspase3) (1:100; Cell Signaling Technology), Pitx3 (1:300; Invitrogen), serotonin (5-HT) (1:1000; Immunostar), and Tubb3 (βIII-tubulin) (1:500; Abcam), polyclonal chicken antisera against green fluorescent protein (GFP) (1:2000; Aves Labs), and polyclonal goat antisera against Sox2 (1:500; Santa Cruz Biotechnology). Monoclonal mouse antibodies were directed against tyrosine hydroxylase (1:600, MAB318; Millipore), Pou4f1 (Brn3a) (1:100; Santa Cruz Biotechnology), Islet1 (Isl1) (1:100; Developmental Studies Hybridoma Bank), Ki67 (1:200; Abcam), and E2F3 (1:100; Millipore). Secondary antibodies were either fluorescently labeled (Alexa Fluor 488/594; Invitrogen) or coupled to biotin/streptavidin–horseradish peroxidase (Jackson ImmunoResearch) and detected using the Vectastain ABC System (Vector Laboratories). Fluorescent images were taken with a confocal laser scanning microscope (FV 1000; Olympus) and processed with Adobe Photoshop CS software.

5-Ethynyl-2′-deoxyuridine labeling. Pregnant dams were injected intraperitoneally with 10 μg of 5-ethynyl-2′-deoxyuridine (EdU; Invitrogen) per gram of body weight on E11.5 or E12.5. Embryos were dissected 2 or 24 h later, fixed, dehydrated, and embedded in paraffin. Paraffin sections (8 μm) were processed using the Click-iT EdU Alexa Fluor 488 Imaging Kit (Invitrogen) according to the instructions of the manufacturer and double labeled with Ki67 and E2F3 antibodies.

Culture and transfection of primary ventral MH cells. Primary ventral MH (vMH) cultures were prepared from E11.5 C57BL/6 mouse embryos as described previously (Peng et al., 2011). Briefly, the basal plate (BP) and FP of the MHR was microdissected and trypsinized in 0.025% trypsin/0.1% DNaseI (Invitrogen) for 5 min at room temperature. Dissociated cells were plated on poly-D-lysine-coated coverslips at a density of 2×10^5 cells per well in a 24-well plate and cultured in DMEM/F-12 medium containing 10% fetal bovine serum (Invitrogen). The medium was switched to DMEM/F-12 containing 2% B27 supplement (Invitrogen) after 18 h, and cells were transfected with *miR-200* sponge vector, *miR-200* overexpression (OE) or the corresponding control vectors, or with Pre-miR miRNA precursor *mmu-miR-200c* (PM11714; Ambion) or Pre-miR miRNA precursor negative control #2 (NG$^{\#2}$; AM17111; Ambion) using Lipofectamine LTX and Plus Reagent (Invitrogen). Medium was changed at 1 d post-transfection (dpt). Cells were fixed in 4% paraformaldehyde for immunostainings or lysed in RIPA buffer for Western blot analyses at 3 dpt. Transfection efficiency of primary cells under these conditions was between 5 and 10%.

Cell counting. Pitx3-expressing (Pitx3$^+$) and Pou4f1$^+$ cells were counted on three anteroposterior (A/P) position-matched coronal midbrain sections, and Isl1$^+$ and 5-HT$^+$ cells were counted on every fifth serial coronal hemisection through the midbrain or hindbrain of E12.5 control and *En1*$^{+/Cre}$; *Dicer1*$^{flox/flox}$; *CAG–CAT–EGFP* embryos. EdU$^+$, Ki67$^+$, Sox2$^+$, and E2F3$^+$ cells were counted on three A/P position-matched coronal hemisections through the ventral MHR of E11.5 and E12.5 control and *En1*$^{+/Cre}$; *Dicer1*$^{flox/flox}$ (*Dicer1 cKO*) embryos. GFP$^+$, Sox2$^+$, Tubb3$^+$, and E2F3$^+$ primary vMH cells were counted in 20 random fields per coverslip, and data were collected from at least three independent experiments.

miRNA profiling of MH tissues and differentiating mouse ESC cultures. Tissues comprising the caudal diencephalon, mesencephalon, and rostral rhombomere 1 were microdissected from E10.5 and E12.5 control (*En1*$^{+/Cre}$; *Dicer1*$^{+/flox}$) and *Dicer1 cKO* embryos (see Fig. 4*A*). Tissues from three embryos were pooled according to genotypes. JM8 (C57BL/6N agouti) mouse ESCs (mESCs) (Pettitt et al., 2009) were cultured and differentiated into glutamatergic neurons following the protocol of Bibel et al. (2007). Samples (cells from a 10-cm-diameter dish or from four wells of a six-well plate) were collected at day 4 (mESCs), day 12 [embryoid bodies (EBs)], and day 20 (neurons) of the differentiation procedure. Successful differentiation of the mESCs into neurons was confirmed in a fraction of the cells by immunostaining for Sox2 and Tubb3 (data not shown). Total RNA was isolated from MH tissues and cell samples using Trizol Reagent (Invitrogen). The small RNA fraction with a size range of 10–40 nt was separated using flashPAGE Fractionator (Ambion) according to the instructions of the manufacturer, ligated with synthetic RNA adapters, reverse transcribed, and amplified using Illumina sequencing primers. The adapter-ligated libraries were se-

Table 1. NGS expression levels (reads) of *miR-200* family members in the MHR of wild-type (Het.) or *Dicer1 cKO* embryos at E10.5 or E12.5

miRNA	E10.5 Het.	E12.5 Het.	E12.5 *Dicer1 cKO*	E12.5 *Dicer1 cKO*/E12.5 Het.	E12.5 Het./ E10.5 Het.
mmu-miR-200a	724	290	4	0.033545	0.400552
mmu-miR-429	402	207	4	0.046995	0.514925
mmu-miR-200b	864	305	8	0.06379	0.353009
mmu-miR-141	280	136	8	0.143058	0.485714
mmu-miR-200c	1699	474	34	0.174447	0.278988

The last two columns indicate the ratios between genotypes or stages.

quenced for 36 cycles on the Illumina/GAII Sequencer according to the instructions of the manufacturer. For the mapping of small RNA sequencing reads, 3′ adapter sequences were first removed from the sequencing reads using an in-house Perl script (Max Delbrück Center). The reads between 17 and 30 nt were retained and mapped to known mouse pre-miRNA sequences deposited in miRBase (version 16.0) (Kozomara and Griffiths-Jones, 2011) without any mismatches using soap.short software (Li et al., 2008). Downregulated miRNAs in the *Dicer1 cKO* embryos were determined by comparing the mutant to the heterozygous (control) samples for each embryonic stage analyzed, after excluding the very-low-abundance miRNAs (<10 sequencing reads in the control sample) from these lists (Table 1).

Vector constructs. For construction of the *miR-200* OE vectors, the *mmu-miR-200c/141* gene cluster (MGI Symbol 3618750) was amplified from C57BL/6 mouse genomic DNA using the primers in Table 2 and inserted into the *pcDNA6.2–EmGFP* vector [Addgene plasmid 22741 (Lau et al., 2008)] downstream of the *EmGFP* sequence to obtain *pcDNA6.2–EmGFP–miR-200c–141* OE vector or cloned together with a *U6* promoter [from *pLL3.7* vector; Addgene plasmid 11795 (Rubinson et al., 2003)] into the *pCAG–EGFP* vector [generated and kindly provided by Dr. D. Refojo, Max Planck Institute of Psychiatry, Munich/Germany] to obtain *pU6–miR-200c–141–CAG–EGFP* OE vector (OE-*miR-200* vector). The *mmu-miR-141* gene was removed from the *pcDNA6.2–EmGFP–miR-200c–141* vector using *Afe*I and *Xho*I restriction sites to obtain *pcDNA6.2–EmGFP–miR-200c* OE vector. Levels of *miR-200c* and *miR-141* expression from the *pcDNA6.2–EmGFP–miR-200c–141*, *pU6–miR-200c–141-CAG–EGFP*, and *pcDNA6.2–EmGFP–miR-200c* OE vectors were quantified by real time RT-PCR after transfection into HEK-293 cells. Expression levels of *miR-200c* and *miR-141* were increased by ~50- and ~1400-fold, respectively, after transfection of the *pcDNA6.2–EmGFP–miR-200c–141* OE vector in HEK-293 cells, and transfection of this vector in primary vMH cultures caused a severe loss of transfected cells compared with the *pcDNA6.2–EmGFP* control-transfected cells (data not shown). This vector was therefore not used for additional experiments. Transfection of the *pcDNA6.2–EmGFP–miR-200c* OE vector in HEK-293 cells resulted in an ~1000-fold increase of *miR-200c* expression but barely detectable *miR-141* levels (data not shown). This vector was therefore not used for *miR-200* OE experiments in primary vMH cultures.

Construction of the *miR-200* sponge vector was done as follows. Because a gene with a 3′UTR containing a fully complementary sequence to the miRNA can inhibit the function of this miRNA (Ameres et al., 2010; Mukherji et al., 2011), oligonucleotides that are fully complementary to the sequences of the five members of the *miR-200* family (Table 2) were synthesized, annealed, ligated, gel purified, and cloned as concatemers into the *pCAG–EGFP* vector to obtain *pCAG–EGFP–8xmiR-200* sponge vector (hereafter named *miR-200* sponge vector).

The mouse *Sox2* 3′UTR (Entrez Gene accession number NM_011443.3) and *E2F3* 3′UTR (Entrez Gene accession number NM_010093.3) were amplified from C57BL/6 mouse genomic DNA using the primer pairs indicated in Table 2 and cloned into the *Xba*I site downstream of the luciferase CDS in the *pGL3 promoter* vector (Promega) to obtain *pGL3–Sox2–3′UTR* and *pGL3–E2F3–3′UTR* sensor vectors. Site-directed mutagenesis of conserved *miR-200c* binding sites (BSs) within the mouse *Sox2* and *E2F3* 3′ UTRs of these sensor vectors was done using the primers listed in Table 2 and the Quickchange Lightning Multi Site-Directed Mutagenesis Kit (Stratagene) according to the instructions of the manufacturer to obtain *pGL3–mut–Sox2–3′UTR* or *pGL3–mut–E2F3–3′UTR* sensor vectors. The distal and proximal promoter regions of the *mmu-miR-200c/141* gene cluster (MGI Symbol 3618750) were amplified from C57BL/6 mouse genomic DNA using the primer pairs in Table 2 and cloned into the *pGL3 basic* vector (Promega) to obtain *pGL3–mmu-miR-200c/141* reporter vectors. *Sox2* (Entrez Gene accession number NM_011443.3) and *E2F3* (Entrez Gene accession number NM_010093.3) CDSs were amplified from E12.5 C57BL/6 mouse brain cDNA using the primer pairs in Table 2 and cloned into *pcDNA3.1* (Invitrogen) to obtain *pcDNA3.1–Sox2* and *pcDNA3.1–E2F3* vectors, respectively.

Transfection efficiency of these vectors in COS-7 and HEK-293 cells was between 80 and 90%.

Luciferase reporter assays. The functionality of *miR-200* OE and *miR-200* sponge vectors was tested in COS-7 cells (expressing low levels of endogenous *miR-200c*; data not shown) cotransfected with 300 ng/well *pGL3–Sox2–3′UTR* sensor vector and 8 ng/well *pRL–SV40* (internal transfection control) along with 600 ng/well *pcDNA6.2–EmGFP–miR-200c–141*, *pcDNA6.2–EmGFP–miR-200c*, *pU6–miR-200c–141–CAG–EGFP* OE vectors or empty control (*pcDNA6.2–EmGFP*) and with or without 600 ng/well *miR-200* sponge vector, using Lipofectamine LTX and Plus Reagent (Invitrogen). The miRNA sensor assays were conducted in COS-7 cells cotransfected with 300 ng/well *pGL3–Sox2–3′UTR* or *pGL3–E2F3–3′UTR* sensor vectors and 10 or 30 nM miRNA precursor *mmu-miR-200c* (PM11714; Ambion) or miRNA precursor NG#2 (AM17111; Ambion) as negative control. The corresponding rescue assays were done in COS-7 cells cotransfected with 300 ng/well *pGL3–mut–Sox2–3′UTR* or *pGL3–mut–E2F3–3′UTR* sensor, 600 ng/well *pcDNA6.2–EmGFP–miR-200c* OE or empty control (*pcDNA6.2–EmGFP*), and 8 ng/well *pRL–SV40* vectors. The *mmu-miR-200c/141* promoter assays were performed in HEK-293 cells cotransfected with 300 ng/well *pGL3–mmu-miR-200c/141* reporter vector and 400 ng/well *pcDNA3.1–Sox2* or *pcDNA3.1–E2F3* plasmids. Cells were lysed in passive lysis buffer 30 h after transfection, and Firefly and Renilla luciferase luminescence were measured in a Centro LB 960 luminometer (Berthold Technologies) using the Dual-Luciferase Reporter Assay system (Promega) according to the instructions of the manufacturers. Firefly luminescence was normalized against Renilla luminescence for each well. Assays were performed in triplicates, and data are derived from three independent experiments.

Quantitative RT-PCR assays. Total RNA was isolated from cultured primary vMH, COS-7, and HEK-293 cells using Trizol Reagent (Invitrogen). One microgram of total RNA was polyadenylated and reverse transcribed using NCode SYBR Green miRNA qRT-PCR Kit (Invitrogen) according to the instructions of the manufacturer. For detection of miRNA expression levels, quantitative RT (qRT)-PCR assays were conducted using the NCode miRNA universal qPCR primer as reverse primer and the specific miRNA forward primers listed in Table 3. The amplification conditions were an initial step at 95°C for 10 min, followed by 45 cycles of 20 s at 95°C and 1 min at 60°C. All assays were performed in triplicate and included negative controls. The threshold cycle (Ct) value was recorded for each reaction, and the expression level of each miRNA was calculated relative to *U6B*, a ubiquitously expressed small nuclear RNA (snRNA). Data are presented as target gene expression = $2^{-\Delta\Delta ct}$, with ΔCt = (target gene Ct − *U6B* Ct) according to the $2^{-\Delta\Delta ct}$ method described previously (Livak and Schmittgen, 2001).

Western blot analyses. Cells were processed as described previously (Peng et al., 2007). Antibodies used were rabbit anti-Tubb3 (1:500; Abcam), goat anti-Sox2 (1:500; Santa Cruz Biotechnology), mouse anti-E2F3 (1:200; Millipore), and mouse anti-Actb (β-actin) (1:2000; Sigma).

Statistics. All values shown are mean ± SEM. Statistical significance between groups was assessed by paired *t* tests or independent-samples *t* tests using the SPSS 10.0 software (SPSS). A value of $p < 0.05$ was considered significant.

Results

Loss of *Dicer1* function in the MHR leads to a progressive loss of midbrain/hindbrain tissues and increased cell death

To understand the role of miRNAs in the development of the murine MHR, we deleted the *Dicer1* gene in this region by gen-

Table 2. Primers and oligos used for vector construction and site-directed mutagenesis

Gene (application)	Forward primer (5′ → 3′)	Reverse primer (5′ → 3′)	Product length (bp)
mmu-miR-200c + *mmu-miR-141* genes (miRNA overexpression)	GCCTCGAGGAAGGCAGCCATTTTGTCTC	GGAGATCTGCCGCTTCTCTTG	708
miR200 oligos for construction of *miR-200* sponge vector	5′-GGATCCACATCGTTACCAGACAGTGTTAGCGTCATCATTACC AGGCAGTATTAGCGTCCATCATTACCCGGCAGTATTAGCGCCAT CTTTACCAGACAGTGTTAGCGACGGCATTACCAGACAGTATTAA GATCT-3′	5′-AGATCTTAATACTGTCTGGTAATGCCGTCGCTAAC ACTGTCTGGTAAAGATGGCGCTAATACTGCCGG GTAATGATGGACGCTAATACTGCCTGGTAAT GATGACGCTAACACTGTCTGGTAACGA TGTGGATCC-3′	These oligos were annealed and cloned as concatemers into *pCAG–EGFP* vector.
mir-200 sponge vector	5′-GGATCCACATCGTTACCAGACAGTGTTAGCGTCATCATTAC CAGGCAGTATTAGCGTCCATCATTACCCGGCAGTATTAGCGCC ATCTTTACCAGACAGTGTTAGCGACGGCATTACCAGACAGTAT TAAGATCCACATCGTTACCAGACAGTGTTAGCGTCATCATTACC AGGCAGTATTAGCGTCCATCATTACCCGGCAGTATTAGCGCCAT CTTTACCAGACAGTGTTAGCGACGGCATTACCAGACAGTATTAA GATCCACATCGTTACCAGACAGTGTTAGCGTCATCATTACCAGGC AGTATTAGCGTCCATCATTACCCGGCAGTATTAGCGCCATCTTTA CCAGACAGTGTTAGCGACGGCATTACCAGACAGTATTAAGATCCA CATCGTTACCAGACAGTGTTAGCGTCATCATTACCAGGCAGTATTA GCGTCCATCATTACCCGGCAGTATTAGCGCCATCTTTACCAGACAG TGTTAGCGACGGCATTACCAGACAGTATTAAGATCCACATCGTTA CCAGACAGTGTTAGCGTCATCATTACCAGGCAGTATTAGCGTCCA TCATTACCCGGCAGTATTAGCGCCATCTTTACCAGACAGTGTTAG CGACGGCATTACCAGACAGTATTAAGATCCACATCGTTACCAGAC AGTGTTAGCGTCATCATTACCAGGCAGTATTAGCGTCCATCATTA CCCGGCAGTATTAGCGCCATCTTTACCAGACAGTGTTAGCGACGG CATTACCAGACAGTATTAAGATCCACATCGTTACCAGACAGTGTT AGCGTCATCATTACCAGGCAGTATTAGCGTCCATCATTACCCGGC AGTATTAGCGCCATCTTTACCAGACAGTGTTAGCGACGGCATTAC CAGACAGTATTAAGATCCACATCGTTACCAGACAGTGTTAGCGTC ATCATTACCAGGCAGTATTAGCGTCCATCATTACCCGGCAGTATT AGCGCCATCTTTACCAGACAGTGTTAGCGACGGCATTACCAGACA GTATTAAGATCT-3′		1038
Sox2 3′ UTR (miRNA sensor assays)	TTAACGCAAAAACCGTGATG	CAAGACCACGAAAACGGTCT	516
Mutant *Sox2* 3′ UTR (*miR-200c* BS)	CGATGAAAAAAAAGTTTTAATATTTGCAAGCAACTTTTGTA*GTGA TAA*TATCGAGATAAACATGGCAATCAAATGTCCATTGTTTATAA		
E2F3 3′ UTR (miRNA sensor assays)	TAAGGGGCTTAACTGGCGTA	ACTCCCAGTGTTGGGAGAAA	736
Mutant *E2F3* 3′ UTR (*miR-200c* BS2)	GTAGTATCTGGCACACAAAGTAGATGAGTACTA*GTCATAA*TTTGT TACTTTAAGTCCTGAGATGCAGGTTCCC		
Mutant *E2F3* 3′ UTR (*miR-200c* BS4)	TGTCGTACATGTAGCTCTGTCTGTAAATAGAATCG*GTCATAA*TAA AGCTTTAGCTTTCAGGAAAAACGAAGTAAGAA		
mmu-miR-200c/141 (Promoter 1)	CACACACAAATTACAAGGGAAAAG	CCTGCAGGCACACAGGTGATGGCCC	144 (−1286 to −1143)
mmu-miR-200c/141 (Promoter 2)	GGATCCAAAGATGGCCTCTTTC	CTCTCGCTCTTCCTCCTTCA	268 (−686 to −419)
Sox2 cDNA (overexpression)	GGCGAATTCATGTATAACATGATGGAGACGGAGC	TCTCGAGAGTCCAGCCCTCACATGTGCGACA	970
E2F3 cDNA (overexpression)	AAGAGCAGGAGCGAGAGATG	GGACAACACTGCGATACACG	1469

Mutated nucleotides are underlined and in italics.

Table 3. Primer and PCR conditions used for qRT-PCR analyses

Gene (application)	Forward primer (5′ → 3′)	Tm (°C)	Cycles
mmu-miR-200c (qRT-PCR)	TAATACTGCCGGGTAATGATGG	60	45
mmu-miR-141 (qRT-PCR)	TAACACTGTCTGGTAAAGATGG	60	45
U6B RNA (qRT-PCR)	CGCAAGGATGACACGCAAATTCG	60	45

erating $En1^{+/Cre}$; $Dicer1^{flox/flox}$ (hereafter referred to as *Dicer1 cKO*) mice. The *Dicer1 cKO* pups died shortly after birth, probably as a result of feeding problems (data not shown). After $En1^{+/Cre}$-mediated recombination of the floxed *Dicer1* alleles at approximately E9.0 (Puelles et al., 2004), *Dicer1* mRNA was not detected within the $En1^{+}$ MHR of the *Dicer1 cKO* mice from E9.5 onward (Fig. 1*A*). Expression of *miR-124*, one of the most abundant miRNAs in the brain (Lagos-Quintana et al., 2002), was already strongly reduced within the $En1^{+}$ domain of the *Dicer1 cKO* embryos at E11.5 and completely lost at E12.5 (Fig. 1*B*), indicating that the loss of Dicer1-mediated processing of pre-miRNAs in the mutants at E9.5 abolishes the expression of mature miRNAs 2–3 d later. In line with this finding, the first morphological changes in the MHR of the *Dicer1 cKO* mice became visible at E12.5. A progressive thinning of the MH neuroepithelium was evident from E12.5 onward, and a progressive loss of dorsal and ventral MH tissues became visible at E14.5 in the *Dicer1 cKO* embryos, resulting in the complete absence of dorsal MH structures, such as the superior/inferior colliculi and the cerebellum, in the postnatal day 0 (P0) *Dicer1 cKO* pups (Fig. 1*C*). Fate-mapping of the $En1^{+}$ and $Dicer1^{+/-}$ or $Dicer1^{-/-}$ cells in $En1^{+/Cre}$; $Dicer1^{+/flox}$ and *Dicer1 cKO* × *CAG–CAT–EGFP* mice showed that $En1^{+}$ (GFP^{+}) cells were almost entirely absent in the dorsal MHR of the mutant mice at P0 (Fig. 1*C*). Apoptotic cell death (assessed by the expression of cCaspase3) was massively increased in the dorsal MHR of the *Dicer1 cKO* embryos from E11.5 onward (Fig. 1*D* and data not shown). Notably, apoptotic cell death was not as pronounced in the ventral MHR of the *Dicer1 cKO* embryos (Fig. 1*D* and data not shown). Altogether, these data indicate that the absence of Dicer1-processed mature miRNAs in the MHR results in a progressive loss of dorsal and ventral MH tissues, which is in part attributable to the reduced survival of the corresponding cells.

Establishment of the MHB and patterning of the MHR are not affected in the *Dicer1 cKO* embryos

The MHR phenotype of the *Dicer1 cKO* mice, although temporally delayed, strongly resembled the MHR phenotype of mouse mutants for the IsO genes *Wnt1* (McMahon and Bradley, 1990), *Fgf8* (Chi et al., 2003), *En1/2* (Wurst et al., 1994; Simon et al.,

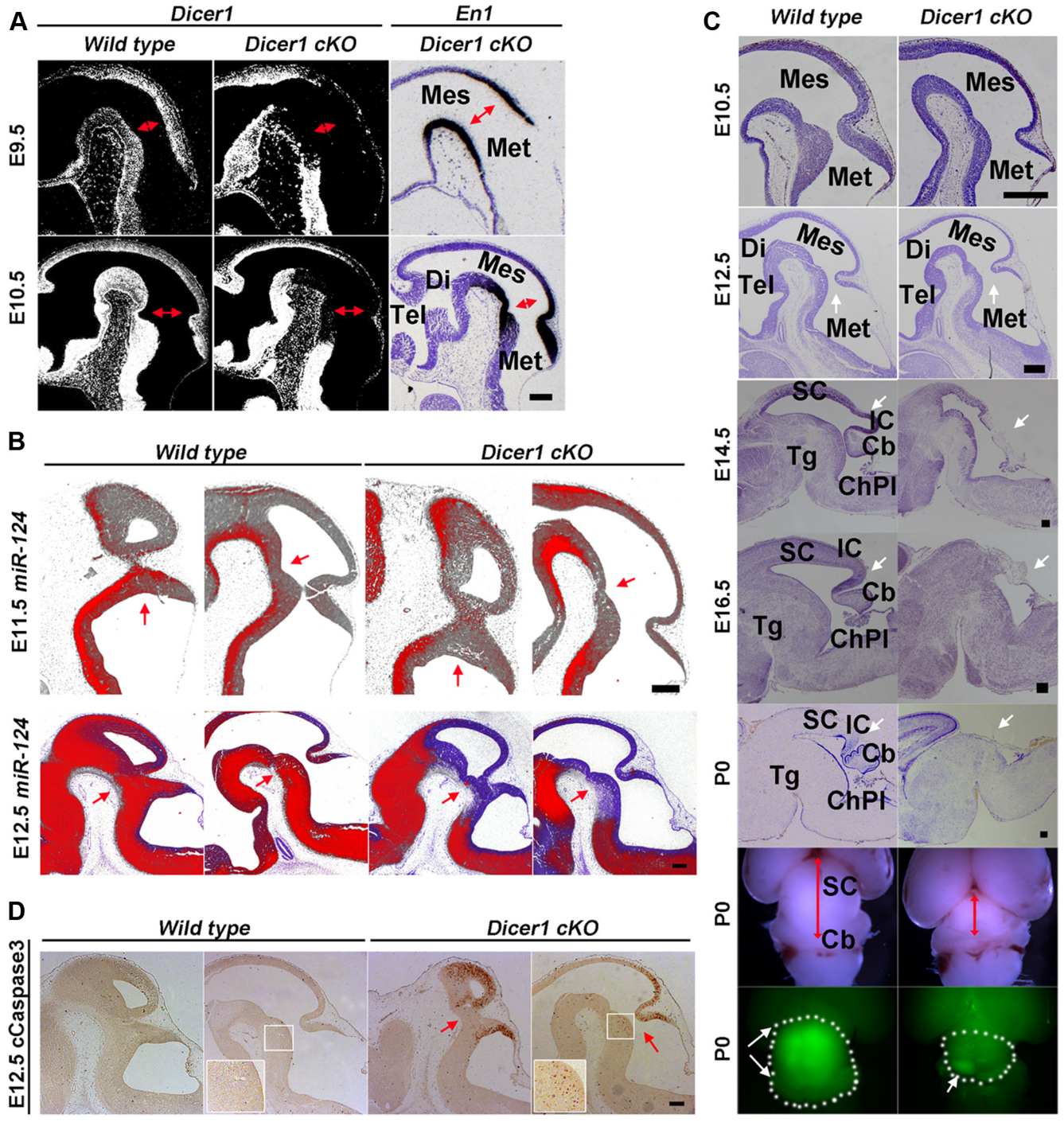

Figure 1. Loss of *Dicer1* function in the MHR leads to a progressive loss of MH tissues and increased cell death. ***A***, *Dicer1* expression was abolished within the *En1*$^{+}$ domain of *Dicer1 cKO* mice from E9.5 onward. Red double arrows mark the approximate position of the MHB. Scale bar, 100 μm. ***B***, Decreased expression at E11.5 and absence at E12.5 of mature *miR-124* in the MHR of *Dicer1 cKO* embryos (red arrows). Scale bar, 100 μm. ***C***, A thinner MH neuroepithelium was apparent at E12.5, and a progressive loss of dorsal and ventral MH tissues became visible in the *Dicer1 cKO* embryos at E14.5, resulting in the complete absence of the midbrain and rostral hindbrain in P0 mutant pups (white arrows). Bottom panels, Dorsal views of the MHR in *En1*$^{+/Cre}$*; Dicer1*$^{+/flox}$*; CAG–CAT–EGFP* (wild-type) and *En1*$^{+/Cre}$*; Dicer1*$^{flox/flox}$*; CAG–CAT–EGFP* (*Dicer1 cKO*) pups at P0, showing the almost complete absence of GFP^{+} (En1^{+}) cells (white arrows) concomitant with a strong reduction of the dorsal MHR (red double arrows and white circles) in the *Dicer1 cKO* mice. Scale bars, 200 μm. ***D***, Massive increase of apoptotic (cCaspase3^{+}) cells in the dorsal MHR, whereas vMH tissues were less affected (red arrows and insets) in the *Dicer1 cKO* embryos at E12.5. Scale bar, 100 μm. Cb, Cerebellum; ChPl, choroid plexus; Di, diencephalon; IC, inferior colliculus; Mes, mesencephalon; Met, metencephalon; SC, superior colliculus; Tel, telencephalon; Tg, tegmentum.

2001), *Lmx1b* (Guo et al., 2007), and *Pax2* (Schwarz et al., 1997). We therefore assessed the expression of these IsO and other A/P (*Otx2*, *Gbx2*) and dorsoventral (D/V) (*Shh*) patterning genes in the *Dicer1 cKO* embryos, but their expression was not altered in the MHR of the mutant embryos at E9.5, E10.5, and E12.5 (Fig. 2*A* and data not shown). Because the protein but not the mRNA expression levels of some of these genes might be affected in the *Dicer1 cKO* embryos and because of the lack of working antibodies for some of the crucial IsO factors, such as Wnt1 and Fgf8, we used an indirect approach to address this issue by detecting known direct target genes and negative modulators of the Fgf8 signaling pathway in the *Dicer1 cKO* embryos. However, the ex-

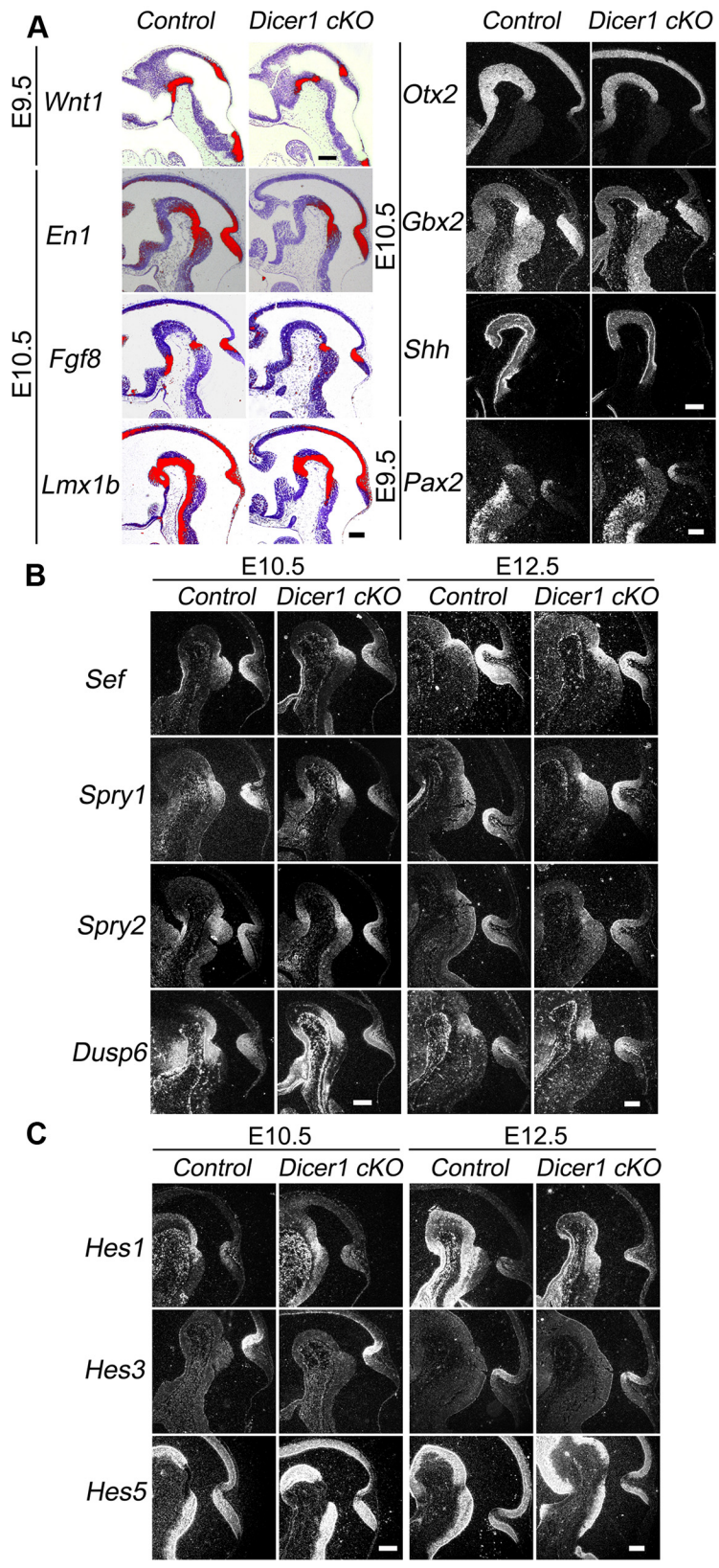

Figure 2. Patterning of the MHR is not affected in *Dicer1 cKO* embryos. ***A***, Expression of the Is0 or FP genes *Wnt1*, *En1*, *Fgf8*, *Lmx1b*, *Otx2*, *Gbx2*, *Shh*, and *Pax2* was not altered in the *Dicer1 cKO* embryos at E9.5 or E10.5 ($n = 3$ embryos/genotype/stage). ***B***, Expression of the direct target genes of the Fgf8 signaling pathway, *Sef1*, *Spry1/2*, and *Dusp6*, was not affected in the *Dicer1 cKO* embryos at E10.5 or E12.5. ***C***, Expression of the anti-neurogenic bHLH TFs *Hes1*, *Hes3*, and *Hes5* was not altered in the *Dicer1 cKO* embryos at E10.5 or E12.5. Scale bar, 200 μm.

pression of *Sef* (*Il17rd*), *Spry1*, *Spry2*, and *Dusp6* (*Mkp3*) (Guillemot and Zimmer, 2011) was also not altered in the MHR of the mutant embryos at E10.5 and E12.5 (Fig. 2*B*). Finally, a loss of MH tissues might result from a precocious differentiation and failure to maintain the MHB as a result of the lack of the anti-neurogenic basic helix–loop–helix (bHLH) *Hes* TFs (Hirata et al., 2001), but again the expression of *Hes1*, *Hes3*, and *Hes5* was not affected in the MHR of the *Dicer1 cKO* embryos at E10.5 and E12.5 (Fig. 2*C*). Our data thus indicate that the A/P and D/V patterning of the MHR and the maintenance of the MHB are not affected by the loss of Dicer1-processed mature miRNAs in this region of the brain.

vMH neural progenitors do not generate the appropriate number of neuronal offspring and fail to exit the cell cycle in the *Dicer1 cKO* embryos

Apoptotic cell death was strongly increased in the dorsal MHR, but ventral neural tissues appeared less affected in the *Dicer1 cKO* mice (Fig. 1). To determine the extent of vMH tissue loss and to establish whether the neuronal populations arising from the ventral MHR [the GFP$^+$ (En1$^+$) domain in *Dicer1 cKO; CAG–CAT–EGFP* embryos] develop normally in the mutant embryos, we assessed the identity and numbers of midbrain dopaminergic (mDA), red nucleus (RN), and oculomotor (OM) neurons residing in the ventral midbrain and of serotonergic (5-HT) neurons residing in the ventral rostral hindbrain. In fact, only ~10% of the Pitx3$^+$ mDA, ~24% of the Pou4f1$^+$ RN neurons, and ~67% of the Isl1$^+$ OM neurons in the ventral midbrain and ~53% of the 5-HT$^+$ neurons in the rostral hindbrain persisted in the *Dicer1 cKO* embryos at E12.5 (Fig. 3*A–U*), the time point when the first subtle morphological alterations were detected in the dorsal MHR of the mutant embryos, indicating that, although these neuronal populations were correctly specified, their progenitors did not generate the appropriate amount of neuronal offspring in the *Dicer1 cKO* embryos. We therefore hypothesized that a failure of vMH neural progenitors to exit the cell cycle and to generate the correct numbers of neuronal progeny might contribute to the loss of vMH neural tissues in the mutant embryos. To test this hypothesis, we injected EdU into pregnant dams at E11.5, 24 h before killing these mice. Colabeling for EdU and Ki67 (a marker for proliferating cells in all phases of the cell cycle) showed that the ratio of EdU/Ki67 double-positive cells per total number of EdU$^+$ cells (i.e., cells that

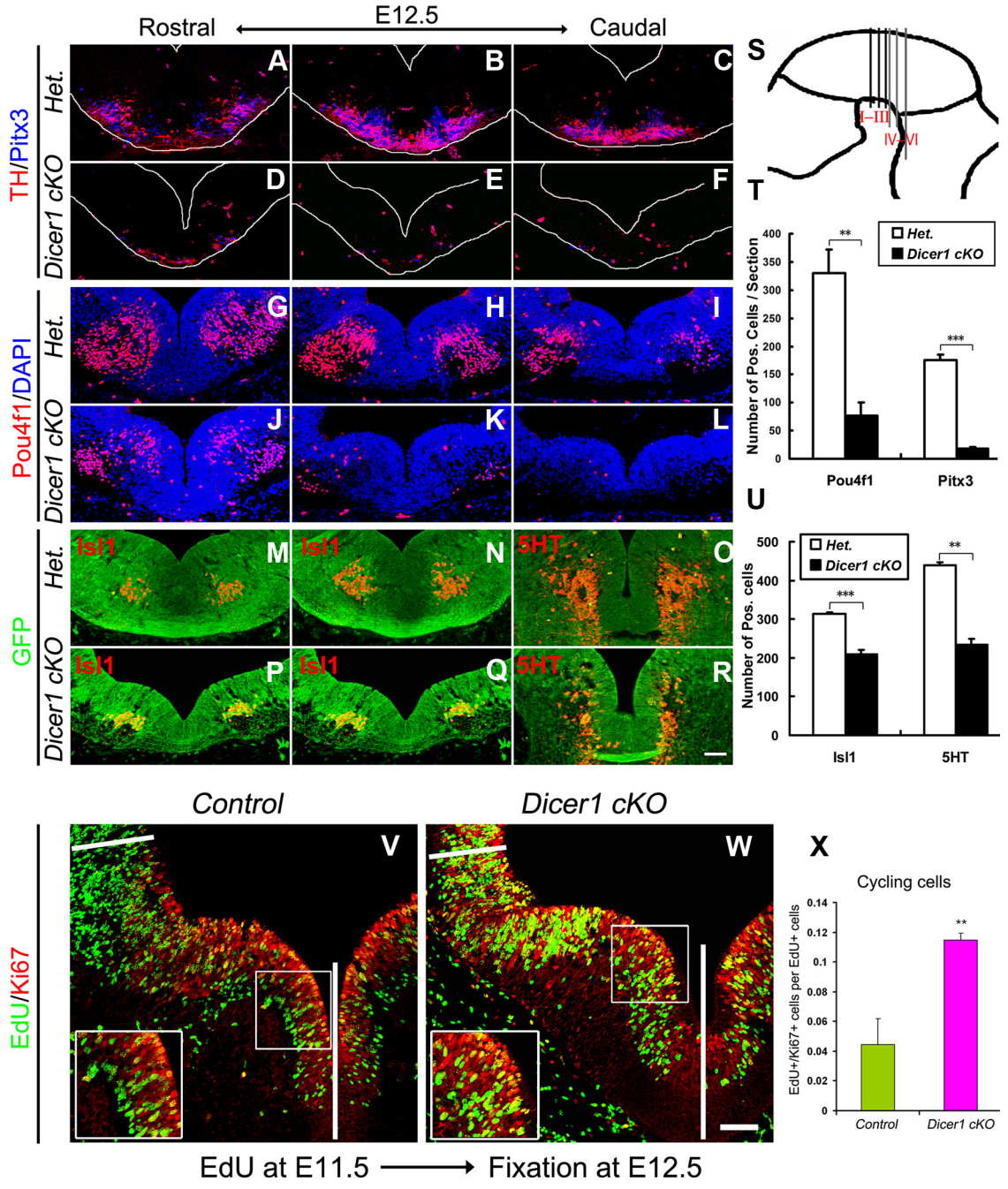

Figure 3. Correct specification but reduced size of vMH neuronal populations attributable to cell-cycle exit defects in the *Dicer1 cKO* embryos. ***A–L***, ***T***, The numbers of Pitx3 $^{+}$ (blue)/TH $^{+}$ (red) mDA and Pou4f1 $^{+}$ (red) RN neurons were drastically reduced in the ventral midbrain of E12.5 *Dicer1 cKO* embryos compared with their heterozygote (Het.) littermates (Pitx3 $^{+}$ cells: Het., 175.89 $\pm$ 9.34; *Dicer1 cKO*, 17.89 $\pm$ 3.42; Pou4f1 $^{+}$ cells: Het., 330.67 $\pm$ 41.79; *Dicer1 cKO*, 76.89 $\pm$ 22.87; $n = 3$; $^{**}p < 0.005$, $^{***}p < 0.001$, independent-samples *t* test). The rostrocaudal position of the sections is depicted in ***S*** by I–III. White lines outline the neuroepithelium. ***M–R***, ***U***, The numbers of Isl1 $^{+}$ (red) OM neurons in the ventral midbrain and of 5-HT $^{+}$ (red) neurons in the ventral rostral hindbrain [mapped by *En1*$^{+/Cre}$-mediated recombination of the *CAG–CAT–EGFP* reporter allele and consequent GFP (green) expression] were diminished in E12.5 *Dicer1 cKO; CAG–CAT–EGFP* embryos compared with their heterozygote (Het.) littermates (Isl1 $^{+}$ cells: Het., 314.33 $\pm$ 4.1; *Dicer1 cKO*, 210 $\pm$ 10.8; 5-HT $^{+}$ cells: Het., 439 $\pm$ 7.22; *Dicer1 cKO*, 233 $\pm$ 16.74; $n = 3$; $^{**}p < 0.005$, $^{***}p = 0.001$, independent-samples *t* test). The rostrocaudal position of the sections is depicted in ***S*** by IV–VI. ***V–X***, Double labeling for EdU (green) (injected at E11.5, 24 h before fixation of the embryos at E12.5) and Ki67 (red) revealed a significant increase of EdU $^{+}$/Ki67 $^{+}$ double-positive cells per total EdU $^{+}$ cells (fraction of cell-cycle reentry) in the ventral MHR of the *Dicer1 cKO* embryos [Control (Het. and WT): 0.0444 $\pm$ 0.0175; *Dicer1 cKO*: 0.1147 $\pm$ 0.0046; $n = 3$; $^{**}p < 0.005$, independent-samples *t* test). White lines delimit the area that was used for quantification of EdU/Ki67 single- and double-positive cells; insets are higher magnifications of the boxed areas in ***V*** and ***W***. Scale bar, 50 μm.

remain in the cell cycle) was remarkably increased by ~2.6-fold in the *Dicer1 cKO* embryos (Fig. 3*V–X*). We concluded that vMH neural progenitors fail to exit the cell cycle and thus to generate the proper amount of postmitotic progeny that can differentiate into mDA, OM, RN, and 5-HT neurons in the *Dicer1 cKO* embryos, thereby contributing to the tissue loss in the absence of a strongly increased cell death in this region of the mutant brain.

miR-200 family members are strongly downregulated in the MHR of the *Dicer1 cKO* mice

miRNAs have been implicated in the regulation of cell proliferation, cell death, and neuronal differentiation in the CNS (Coolen and Bally-Cuif, 2009), but their role in the control of cell-cycle exit of neural progenitors is less well established. To find candidate miRNAs that might target known regulators of cell-cycle

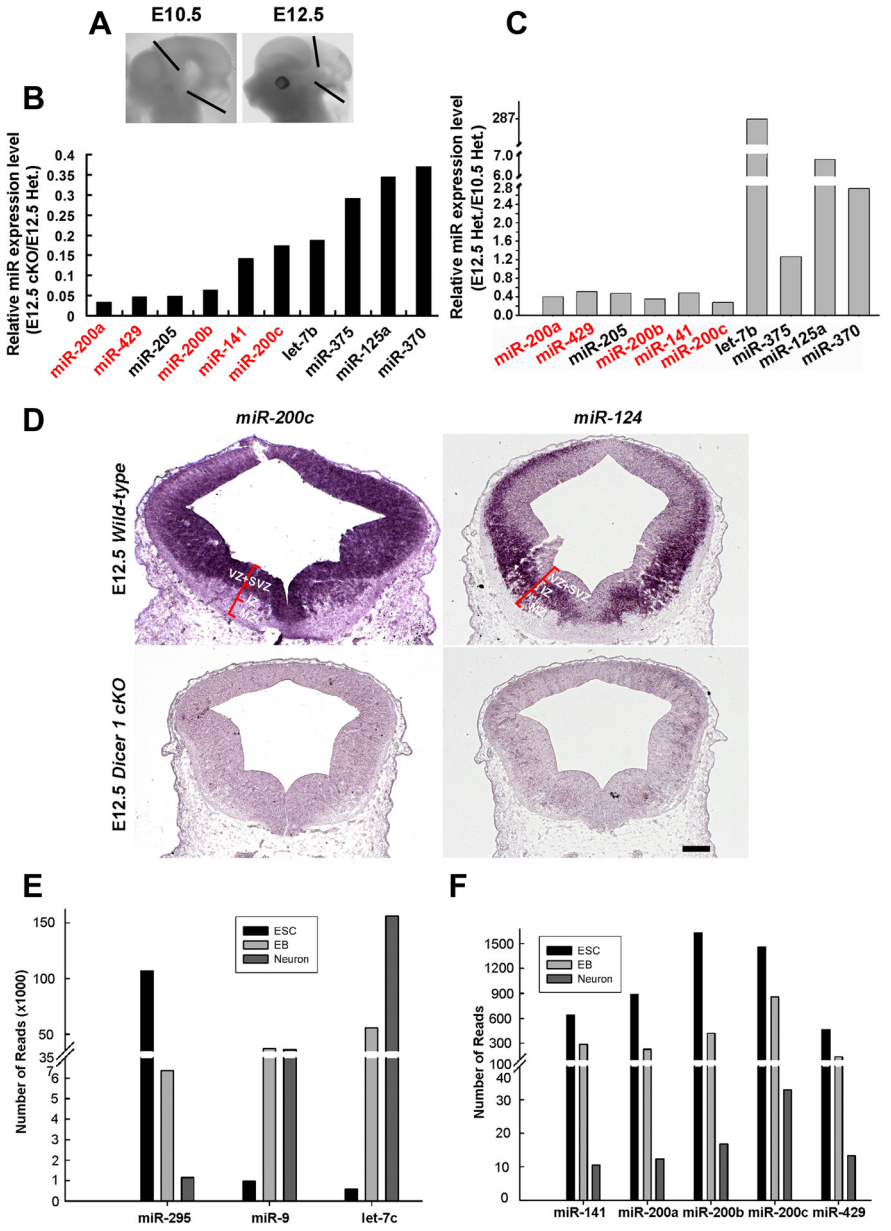

Figure 4. Loss of *miR-200* family members in the MHR of *Dicer1 cKO* embryos. ***A***, The caudal diencephalon, mesencephalon, and rostral rhombomere 1 (delimited by black lines) was dissected from E10.5 and E12.5 wild-type and *Dicer1 cKO* embryos and used for NGS miRNA profiling. ***B***, The five *miR-200* family members (*miR-200a*, *miR-429*, *miR-200b*, *miR-141*, and *miR-200c*, highlighted in red) were among the top 10 most downregulated miRNAs in the MHR of the *Dicer1 cKO* embryos compared with the $En1^{+/Cre}$; $Dicer1^{+/flox}$ (Het.) embryos at E12.5. For values, see Table 1. ***C***, The expression levels of the *miR-200* family (*miR-200a*, *miR-429*, *miR-200b*, *miR-141*, and *miR-200c*, highlighted in red) in $En1^{+/Cre}$; $Dicer1^{+/flox}$ (Het.) embryos were strongly downregulated in the MHR at E12.5 compared with E10.5. For values, see Table 1. ***D***, *miR-200c* is expressed in the VZ, SVZ, and IZ of the MH neuroepithelium in a complementary pattern to *miR-124*, which is strongly expressed in the IZ and MZ. *miR-200c* has a similar expression pattern in the forebrain and hindbrain (data not shown). Expression of *miR-200c* and *miR-124* was abolished in the *Dicer1 cKO* embryos at E12.5. Scale bar, 100 μm. ***E***, NGS profiling of miRNAs expressed during the directed differentiation of mESCs into neurons according to the protocol by Bibel et al. (2007). Known ESCC miRNAs (*miR-295*) or neural-specific miRNAs (*miR-9* and *let-7c*) were selectively enriched in the corresponding steps of the differentiation procedure. ***F***, Expression of all five *miR-200* family members was highest in undifferentiated mESCs and decreased to lowest levels in differentiated neurons. Neuron, Differentiated neurons.

progression and neural progenitor maintenance, we first determined the miRNA expression profile in the MHR (also including some wild-type tissue beyond the $En1^{+}$ domain; Fig. 4*A*) of the E12.5 *Dicer1 cKO* embryos compared with their $En1^{+/Cre}$; $Dicer1^{+/flox}$ heterozygous littermates, using next generation sequencing (NGS) technology. Among the most strongly downregulated miRNAs in the mutant MHR were the five members of the *miR-200* family (*miR-200a/b/c*, *141*, and *429*; Fig. 4*B*). The *miR-200* family was also expressed at lower levels in the MHR of $En1^{+/Cre}$; $Dicer1^{+/flox}$ heterozygous embryos at E12.5 compared with E10.5, whereas *let-7b* and *miR-125a*, two members of the *let-7* and *miR-125* families promoting neuronal differentiation (Coolen and Bally-Cuif, 2009), were strongly upregulated in the MHR of the E12.5 compared with the E10.5 heterozygous embryos (Fig. 4*C*), suggesting that the expression of the *miR-200* family declines with the progression of neuronal differentiation in the MHR. Based on our NGS data (Fig. 4*B*, Table 1), *miR-200c* still showed the highest expression levels in the mutant MHR relative to the other *miR-200* family members at E12.5, and we therefore detected this miRNA in wild-type and *Dicer1 cKO* embryos using LNA-based ISH. In the E12.5 wild-type embryo, *miR-200c* is strongly expressed in the ventricular (VZ), subventricular (SVZ), and intermediate (IZ) zones but not in the mantle zone (MZ) of the MH neuroepithelium (Fig. 4*D*). The expression of *miR-200c* was complementary to the transcription of the neuron-specific *miR-124* (Coolen and Bally-Cuif, 2009) in the IZ and MZ of the E12.5 wild-type embryo (Fig. 4*D*). Notably, *miR-200c* was undetectable and *miR-124* was barely detectable in the MHR of the *Dicer1 cKO* embryos at E12.5 (Fig. 4*D*), thus validating our NGS approach and confirming the near-complete ablation of mature miRNAs in the MHR of the E12.5 *Dicer1 cKO* embryos.

The *miR-200* family members might be generally implicated in the regulation of cell proliferation, cell-cycle exit, and differentiation of pluripotent/multipotent stem cells, including neural stem/progenitor cells (Peter, 2009). To establish whether this is the case, we used an *in vitro* paradigm to differentiate mESCs into $Tubb3^{+}$ postmitotic neurons (Bibel et al., 2007) and determined the miRNA profile in these cells at three different stages of the differentiation protocol: mESCs representing the initial pluripotent state, EBs representing neuroectodermal commitment, and postmitotic neurons representing the differentiated neuron state. Known miRNAs were enriched at the expected stages of the differentiation procedure (Fig. 4*E*), such as the ESCC *miR-295* in the undifferentiated mESC stage (Wang et al., 2008; Martinez and Gregory, 2010), *miR-9* in the committed neuroectodermal and differentiated neuron stage, and *let-7c* in the differentiated neuron stage (Krichevsky et al., 2006; Coolen and Bally-Cuif, 2009), thus validating our approach. Consistent

with a previous report (Gill et al., 2011), expression of the *miR-200* family was highest in undifferentiated mESCs; their expression levels decreased to an intermediate level in committed neuroectodermal cells and dropped to their lowest levels (~30- to 100-fold lower than in the mESCs) in the differentiated neurons (Fig. 4*F*). Notably, *miR-200c* still showed the highest expression level in differentiated neurons among all *miR-200* family members (Fig. 4*F*). We concluded that the *miR-200* family members are highly expressed in undifferentiated pluripotent/multipotent stem/progenitor cells and that their expression levels decline along the commitment and differentiation of these cells into neurons both *in vivo* and *in vitro*. Their strong downregulation in the MHR of the *Dicer1 cKO* embryos might thus contribute to the defective cell-cycle exit and differentiation of vMH neural progenitors observed in these mutants.

Sox2$^+$ and E2F3$^+$ neural progenitor cells accumulate in the MHR of the *Dicer1 cKO* embryos

We next searched for possible targets of the *miR-200* family whose deregulation in MH tissues might cause the cell-cycle defects observed in the *Dicer1 cKO* embryos. Two of the predicted targets of the *miR-200* family using bioinformatics tools (Targetscan; http://www.targetscan.org) are the TFs Sox2 and E2F3. Sox2 is required for the maintenance of self-renewing neural stem/progenitor cells (Graham et al., 2003; Pevny and Nicolis, 2010), and E2F3 plays a pivotal role in cell-cycle progression, particularly in promoting the S-phase entry of proliferating cells (Leone et al., 1998; DeGregori, 2002). Both TFs were expressed in the MHR of E12.5 wild-type mice within the same domain as *miR-200c*: Sox2 expression was confined to the neural progenitors in the VZ/SVZ, whereas E2F3 was expressed in single cells that extended from the VZ/SVZ into the IZ of the ventral MHR and spared the cell layer immediately adjacent to the third ventricle (Fig. 5*A*). Because the Sox2$^+$ and E2F3$^+$ cells appeared to be increased in the ventral MHR of the *Dicer1 cKO* embryos (Fig. 5*A*), we hypothesized that these two TFs might indeed be direct targets of the *miR-200* family in vMH neural progenitors.

To establish this in more detail, we determined the numbers of Sox2$^+$, E2F3$^+$, and proliferating S-phase (EdU$^+$) cells in the MHR of the mutant embryos compared with their wild-type littermates. We focused our analyses on the ventral MHR because this was the region where we had previously detected the cell-cycle exit defects in the *Dicer1 cKO* embryos and because of the massive cell death in the mutant dorsal MHR from E11.5 onward. At E10.5, the Sox2$^+$ domain was not obviously altered, but the Tubb3$^+$ postmitotic neuron domain was clearly reduced in the ventral MHR of the *Dicer1 cKO* embryos (Fig. 5*B*), indicating that the differentiation of neural progenitors into postmitotic neurons was affected in the mutant embryos at or even before E10.5. At E11.5, the Sox2$^+$ domain was visibly expanded at the expense of the Tubb3$^+$ domain (Fig. 5*B*), and the numbers of Sox2$^+$, E2F3$^+$ (G_1/S-phase), and EdU$^+$ (S-phase) neural progenitors were increased by 25% (Sox2$^+$/E2F3$^+$ cells) and 18% (EdU$^+$ cells) in the ventral MHR of the *Dicer1 cKO* embryos (data not shown). At E12.5, the numbers of Sox2$^+$, EdU$^+$, and E2F3$^+$ neural progenitor cells were increased by 1.7- to 1.9-fold, and the thinning of the Tubb3$^+$ domain became even more evident in the ventral MHR of the *Dicer1 cKO* embryos (Fig. 5*C*,*D*,*F*). The increase of Sox2$^+$ cells was attributable to the enlargement of the Sox2$^+$ area and not an increase of Sox2$^+$ cell density in the mutant embryos (Fig. 5*E*). Remarkably, the proportion of EdU$^+$ (S-phase) cells that coexpressed E2F3 (EdU/E2F3 double-positive cells per total amount of EdU$^+$ cells) and the number of EdU/E2F3 double-positive cells were increased by 80% and two-fold, respectively, in the ventral MHR of the *Dicer1 cKO* embryos compared with their wild-type littermates at E12.5 (Fig. 5*G*). The expansion of the proliferating Sox2$^+$ and E2F3$^+$ neural progenitor domain in the ventral MHR of the *Dicer1 cKO* embryos was accompanied by an apparent change of vMH morphology and mediolateral expansion of the cavity of the third ventricle in the mutant embryos (Fig. 5*A–C*). Altogether, our results indicated that proliferating (EdU$^+$/Sox2$^+$/E2F3$^+$) neural progenitors accumulate over time in the ventral MHR of the *Dicer1 cKO* embryos, suggesting that their failure to exit the cell cycle and to generate the proper amount of Tubb3$^+$ neuronal progeny was attributable to their inability to downregulate Sox2 and in particular E2F3 protein levels in the absence of *miR-200* miRNAs.

miR-200 miRNAs promote the neuronal differentiation of vMH neural progenitors

Our results so far suggested that the *miR-200* family might regulate the cell-cycle exit and neuronal differentiation of vMH neural progenitors by targeting the expression of Sox2 and E2F3 in these cells. To establish this more conclusively, we generated an *miR-200* OE vector for the constitutive expression of *miR-200* family members in primary cultures derived from the ventral MHR of E11.5 wild-type mice. We focused on the *miR-200c/141* cluster (located on chromosome 6 in the mouse), because this cluster represents both seed sequence subgroups (that differ by just 1 nt) of the *miR-200* family with potentially different target mRNAs (Peter, 2009; Uhlmann et al., 2010). Overexpression of the *miR-200c/141* cluster under the control of the *U6* promoter (*pU6–miR-200c–141–CAG–EGFP* OE vector or OE-*miR-200* vector; Fig. 6*A*) resulted in a moderate increase (between 1.3- and 2.7-fold) of *miR-200c* and *miR-141* levels in the transfected cells (Fig. 6*B*). Cotransfection of the OE-*miR-200* vector with a *Sox2 3′UTR* sensor vector containing one *miR-200c* BS showed that this vector was able to repress the expression of luciferase from the sensor vector (Fig. 6*C*). Overexpression of *miR-200c/141* in primary vMH cultures led to a significant reduction of Sox2$^+$ and E2F3$^+$ neural progenitor cells and to a significant increase of Tubb3$^+$ postmitotic neurons at 3 dpt (Fig. 6*D–G*). Transfection of an *mmu-miR-200c* pre-miRNA into primary vMH cultures also resulted in a strong reduction of Sox2 and E2F3 and an increase of Tubb3 protein levels in these cultures compared with the control-treated cultures (Fig. 6*H*). These data show that the overexpression of *miR-200* family members indeed promotes the neuronal differentiation of vMH progenitor cells by downregulating the expression of Sox2 and E2F3 in these cells.

We next investigated whether the knockdown of the *miR-200* family in primary vMH cultures leads to the opposite effect, i.e., reduced neuronal differentiation of vMH progenitor cells, thereby mimicking the phenotype observed in the ventral MHR of the *Dicer1 cKO* embryos. To test this, we generated an *miR-200* sponge vector (Ebert et al., 2007) containing eight repeats of a fully complementary sequence to all five *miR-200* family members inserted downstream of the *EGFP* CDS and driven by the *CAG* promoter (Fig. 7*A*). The functionality of this sponge vector was tested by cotransfecting this vector together with the OE-*miR-200* vector and a *Sox2 3′UTR* sensor vector into COS-7 cells. The reduction of luciferase expression from the sensor vector after cotransfection of the OE-*miR-200* vector was in fact abolished (rescued) by the cotransfected *miR-200* sponge vector (Fig. 7*B*). Because primary vMH cells express rather low levels of *miR-200c* compared with the ubiquitously expressed *U6B* snRNA (Fig. 7*C*), we expected that transfection of the *miR-200* sponge vector

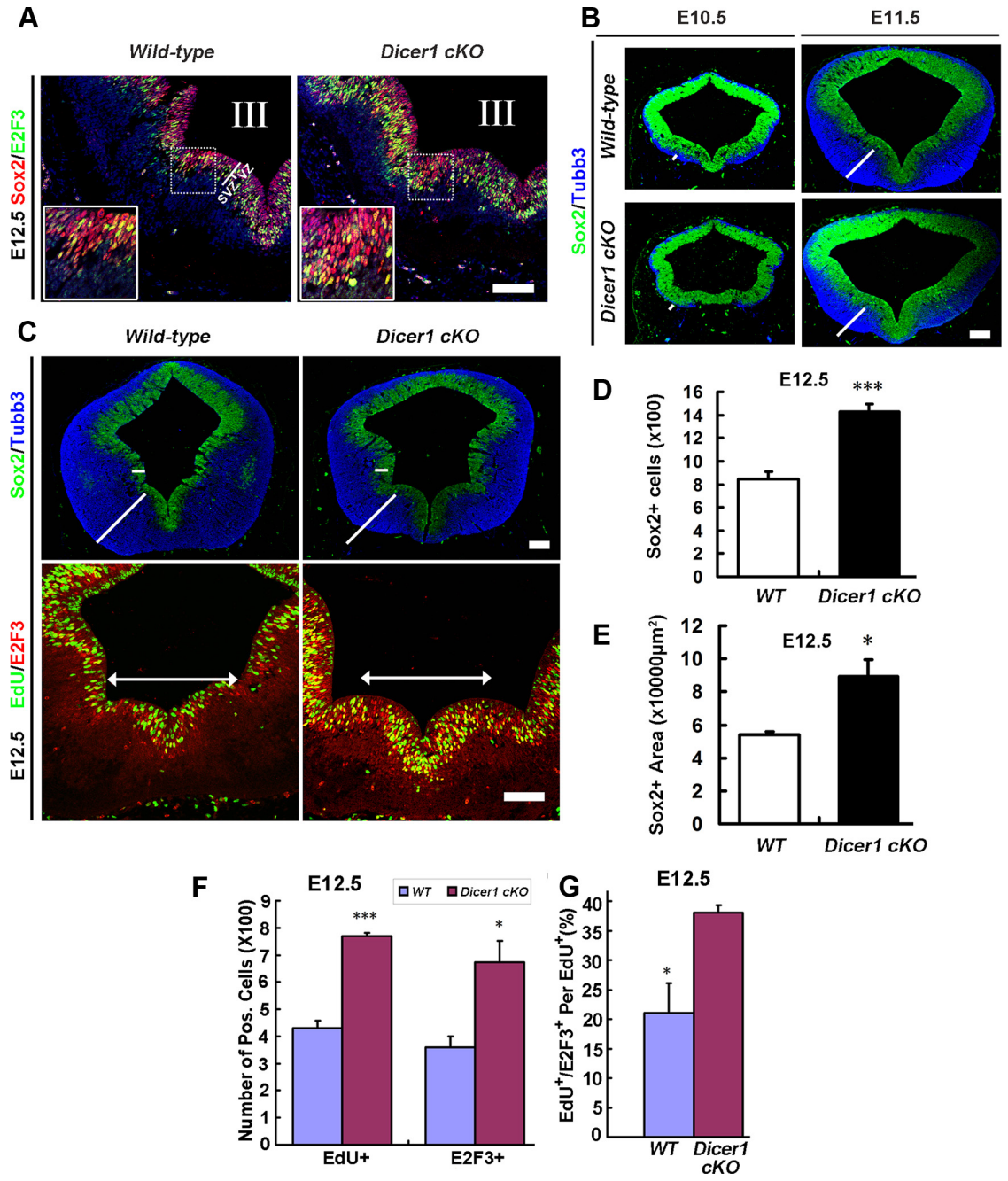

Figure 5. Accumulation of proliferating Sox2 $^+$/E2F3 $^+$ neural progenitors and reduced neuronal differentiation in the ventral MHR of the *Dicer1 cKO* embryos. ***A***, The predicted *miR-200c* targets Sox2 and E2F3 are expressed in the VZ/SVZ and IZ of the MH neuroepithelium. E2F3 is expressed in single cells sparing the layer immediately adjacent to the third ventricle (III). Pictures are taken from adjacent sections to the ones shown in Figure 4 *D*. ***B***, Reduced thickness [white lines correspond to wild-type (WT) embryos] of the Tubb3 $^+$ (blue) postmitotic neuron layer and expansion of the Sox2 $^+$ (green) cell layer in the ventral MHR of the *Dicer1 cKO* embryos at E10.5 and E11.5. ***C***, E12.5 *Dicer1 cKO* embryos have an expanded Sox2 $^+$ (green in top row) and reduced Tubb3 $^+$ (blue) domain [white lines depict the thickness of the corresponding layer in wild-type (WT) embryos] and strongly increased numbers of Sox2 $^+$, E2F3 $^+$ (red), and EdU $^+$ (green in bottom row) neural progenitor cells in the ventral MHR. Note the mediolateral broadening of the ventricular cavity in the ventral MHR of the *Dicer1 cKO* embryos (white double arrows). ***D–F***, Quantification of Sox2 $^+$, EdU $^+$, and E2F3 $^+$ cells in the *Dicer1 cKO* embryos at E12.5. [Sox2 $^+$ cells (***D***): WT, 845.75 $\pm$ 67.45; *Dicer1 cKO*, 1433 $\pm$ 59.16; ***$p = 0.001$; Sox2 $^+$ area (***E***): WT, 53,941.75 $\pm$ 1945; *Dicer1 cKO*, 89,127.75 $\pm$ 10,292; *$p < 0.05$; $n = 4$; EdU $^+$ cells (***F***): WT, 430 $\pm$ 27.4; *Dicer1 cKO*, 770 $\pm$ 10.6; ***$p < 0.001$; E2F3 $^+$ cells (***F***): WT, 360 $\pm$ 39.3; *Dicer1 cKO*, 673 $\pm$ 78.5; *$p < 0.05$; $n = 3$, statistical significance was estimated by independent-samples *t* test.] ***G***, The number of EdU $^+$/E2F3 $^+$ double-labeled cells and their ratio per total amount of EdU $^+$ (S-phase) cells were strongly increased in the ventral MHR of the E12.5 *Dicer1 cKO* embryos [EdU $^+$/E2F3 $^+$ cell numbers: WT, 96 $\pm$ 23.4; *Dicer1 cKO*, 293.7 $\pm$ 13.3; EdU $^+$/E2F3 $^+$ per EdU $^+$ cells (%): WT, 21 $\pm$ 5.1; *Dicer1 cKO*, 38.1 $\pm$ 1.2; $n = 3$, *$p < 0.05$ independent-samples *t* test]. Scale bars: ***A–C***, 100 μm.

would fully knock down the *miR-200* family in these cells. Indeed, the numbers of Sox2 $^+$ and E2F3 $^+$ neural progenitor cells were increased, and the numbers of Tubb3 $^+$ postmitotic neurons were decreased after transfection of the *miR-200* sponge vector compared with the control-transfected primary vMH cells (Fig. 7*D–G*), thus phenocopying the ventral MHR defects of the *Dicer1 cKO* embryos (Fig. 5). In summary, our data strongly support the idea that the *miR-200* family is required to promote the cell-cycle exit and neuronal differentiation of proliferating vMH neural progenitors by targeting the expression of Sox2 and E2F3 in these cells and that the ventral MHR phenotype of the *Dicer1 cKO* mice is mainly caused by the loss of mature *miR-200* miRNAs in these mutants.

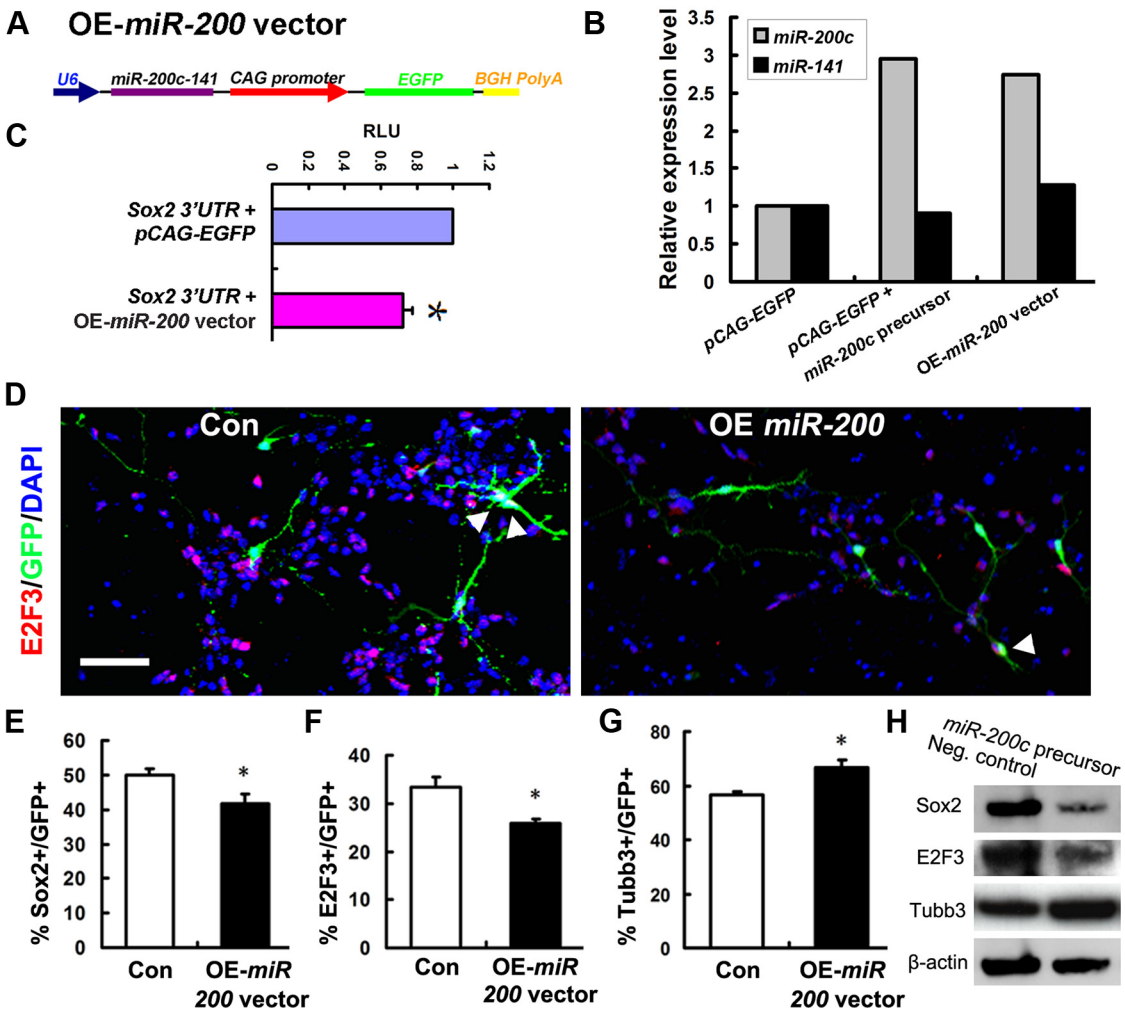

Figure 6. Overexpression of *miR-200c–141* promotes neuronal differentiation of vMH neural progenitors *in vitro*. ***A***, Schematic of the *pU6 –miR-200c–141–CAG–EGFP* OE vector (OE-*miR-200* vector) used for all *miR-200* OE experiments. Expression of the *mmu-miR-200c–141* cluster was under control of an *U6* promoter and was monitored by *CAG* promoter-driven EGFP expression. ***B***, Quantification of the *miR-200c* and *miR-141* expression levels by qRT-PCR after cotransfection of *pcDNA6.2–EmGFP* (*pCAG–EGFP*) vector and the *mmu-miR-200c* precursor miRNA or after transfection of the OE-*miR-200* vector into HEK-293 cells. Transfection of *pCAG–EGFP* "empty" vector alone served as control, and this value was set as 1. Cotransfection of *pCAG–EGFP* and *mmu-miR-200c* precursor miRNA resulted in an increase of only *miR-200c* but not of *miR-141* expression, demonstrating the specificity of the qRT-PCR detection assay. A modest (1.3- to 2.7-fold) increase of *miR-200c* and *miR-141* expression levels was detected after transfection of the OE-*miR-200* vector. ***C***, Functional validation of the OE-*miR-200* vector. Cotransfection of the *pGL3–Sox2–3′UTR* sensor vector and OE-*miR-200* vector in COS-7 cells resulted in a significant repression of luciferase expression from the sensor vector. Cotransfection of *pGL3–Sox2–3′UTR* sensor and *pCAG–EGFP* "empty" vector served as control, and this value was set as 1. (*pGL3–Sox2–3′UTR* + OE-*miR-200* vector: 0.722 ± 0.054, $n = 3$; $^*p < 0.05$, statistical significance was estimated by paired-samples *t* test). RLU, Relative luciferase units. ***D***, Overexpression of *miR-200c–141* caused a decrease of Sox2$^+$ (data not shown) and E2F3$^+$ (red) neural progenitor cells and an increase of Tubb3$^+$ (data not shown) postmitotic neurons in E11.5 primary vMH cultures transfected with the OE-*miR-200* vector [GFP$^+$ (green) cells]. Transfection of *pCAG–EGFP* "empty" vector alone served as control (Con). White arrowheads point at E2F3$^+$ and GFP$^+$ double-labeled cells. Scale bar, 50 μm. ***E–G***, Quantification of Sox2$^+$ (***E***), E2F3$^+$ (***F***), and Tubb3$^+$ (***G***) transfected (GFP$^+$) primary vMH cells after *miR-200* OE. [Sox2$^+$/GFP$^+$ cells (***E***): control, 49.997 ± 1.89; OE-*miR-200* vector, 41.837 ± 2.59; E2F3$^+$/GFP$^+$ cells (***F***): control, 33.453 ± 2.07; OE-*miR-200* vector, 25.888 ± 0.83; Tubb3$^+$/GFP$^+$ cells (***G***): control, 56.504 ± 1.12; OE-*miR-200* vector, 66.639 ± 2.67; $n = 4$; $^*p < 0.05$, independent-samples *t* test). ***H***, Transfection of *mmu-miR-200c* precursor miRNA in primary vMH cells strongly downregulated Sox2 and E2F3 and upregulated Tubb3 protein levels in these cells compared with cells transfected with a negative control precursor miRNA (Neg. control).

Sox2 and *E2F3* mRNAs are direct targets of *miR-200c*

Given the strong correlation between the overexpression or downregulation of *miR-200* miRNAs and the decrease or increase of Sox2$^+$ and E2F3$^+$ cells, respectively, *in vivo* and *in vitro*, we next determined whether Sox2 and E2F3 mRNAs are direct targets of the *miR-200* family. Using bioinformatics prediction tools (http://www.targetscan.org), we found that there is one conserved (among vertebrates) BS for the *miR-200b/c/429* seed sequence subgroup within the mouse *Sox2 3′UTR* and four conserved (in mammals) BSs for the *miR-200* family (two BSs for each seed sequence subgroup) within the mouse *E2F3 3′UTR* (Fig. 8*A*,*B*). We therefore cloned the mouse *Sox2 3′UTR* (containing the single *miR-200c* BS) or *E2F3 3′UTR* (containing two *miR-200c* BSs) into a luciferase reporter (sensor) vector and cotransfected these vectors together with an *mmu-miR-200c* precursor miRNA into COS-7 cells. The *miR-200c* pre-miRNA repressed the luciferase expression from the *Sox2 3′UTR* sensor vector by ~50% and from the *E2F3 3′UTR* sensor vector by ~30% (Fig. 8*C*,*D*). To confirm this result, we cotransfected the *pcDNA6.2–EmGFP–miR-200c* OE vector together with the sensor vectors into COS-7 cells. Luciferase expression was decreased by ~26% (*Sox2 3′UTR*) and ~33% (*E2F3 3′UTR*) after *miR-200c* overexpression, and this repression was abolished after site-directed mutagenesis of the conserved *miR-200c* BSs in the sensor vectors (Fig. 8*A*,*B*,*E*,*F*). Notably, the luminescence values after site-directed mutagenesis of the conserved *miR-200c* BSs were even

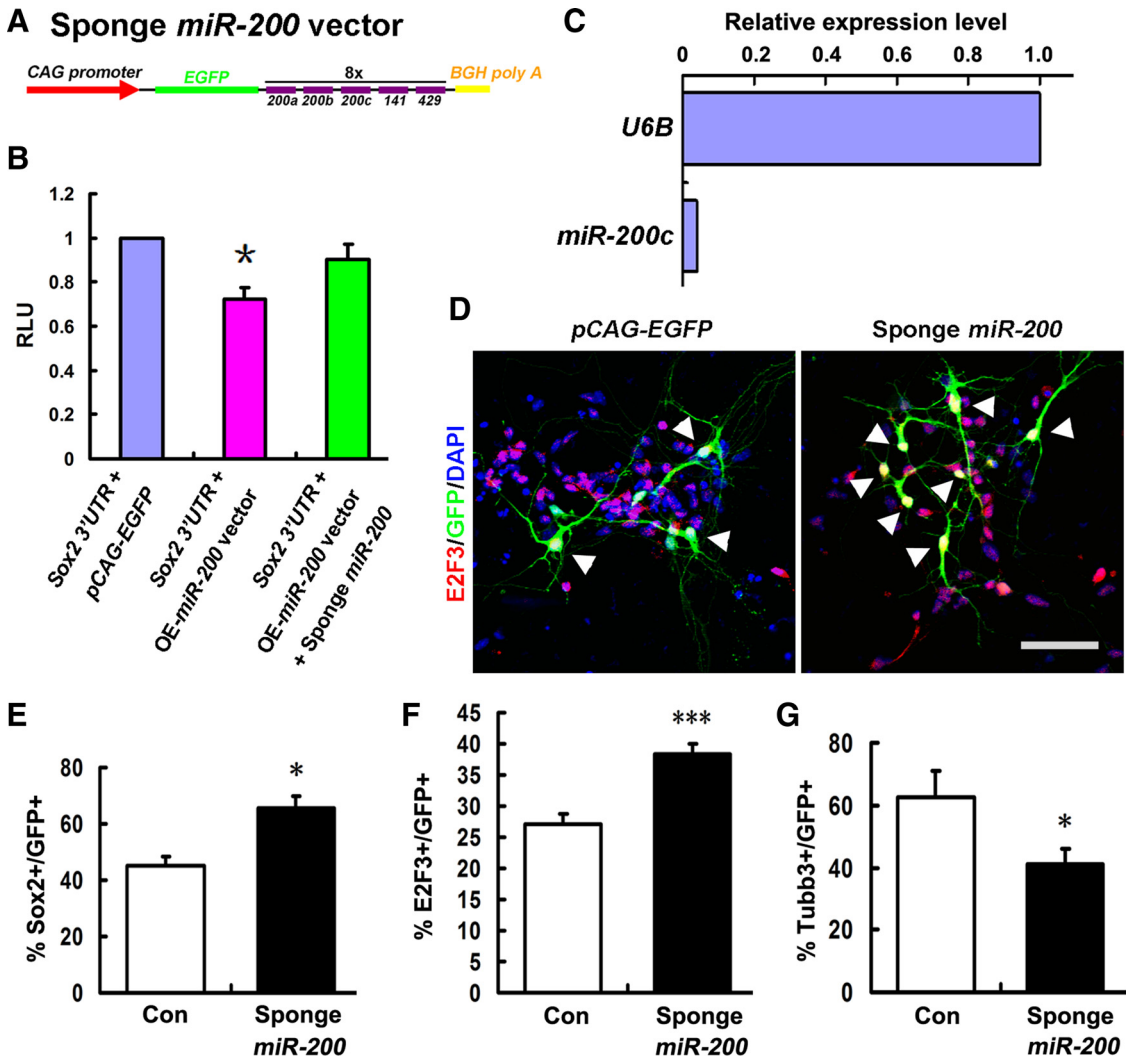

Figure 7. Knockdown of the *miR-200* family suppresses neuronal differentiation of vMH neural progenitors *in vitro*. ***A***, Schematic of the sponge *miR-200* vector. Eight repeats of fully complementary sequences to all five *mmu-miR-200* family members were inserted downstream of the *CAG* promoter-driven *EGFP* CDS in the sponge vector. ***B***, Cotransfection of the *pGL3–Sox2–3′ UTR* sensor vector, OE-*miR-200* vector, and sponge *miR-200* vector in COS-7 cells significantly rescued the luciferase expression from the sensor vector to similar levels as after cotransfection of sensor and *pCAG–EGFP* (control) vectors (value was set to 1) and compared with the cotransfection of sensor and OE-*miR-200* vectors alone (see Fig. 6*C*). (*pGL3–Sox2–3′ UTR* + OE-*miR-200* vector + sponge *miR-200* vector: 0.903 ± 0.069, $n = 3$, $^*p < 0.05$, statistical significance was estimated by paired-samples *t* test). RLU, Relative luciferase units. ***C***, Quantification of endogenous *miR-200c* levels in primary vMH cultures after 4 d *in vitro* by qRT-PCR. *miR-200c* expression levels are $^1/_{25}$ of the *U6B* snRNA levels in these cultures. ***D***, Knockdown of the *miR-200* family in E11.5 primary vMH cells transfected with the sponge *miR-200* vector [GFP$^+$ (green) cells] resulted in an increase of Sox2$^+$ (data not shown) and E2F3$^+$ (red) neural progenitor cells and a decrease of Tubb3$^+$ (data not shown) postmitotic neurons. Transfection of *pCAG–EGFP* "empty" vector alone served as control (Con). White arrowheads point to E2F3$^+$ and GFP$^+$ double-labeled cells. Scale bar, 50 μm. ***E–G***, Quantification of Sox2$^+$ (***E***), E2F3$^+$ (***F***), and Tubb3$^+$ (***G***) transfected (GFP$^+$) primary vMH cells after *miR-200* knockdown. [Sox2$^+$/GFP$^+$ cells (***E***): control, 44.928 ± 3.25; sponge *miR-200* vector, 65.511 ± 4.16; E2F3$^+$/GFP$^+$ cells (***F***): control, 27.183 ± 1.67; sponge *miR-200* vector, 38.255 ± 1.82; Tubb3$^+$/GFP$^+$ cells (***G***): control, 62.63 ± 8.6; sponge *miR-200* vector, 41.13 ± 4.93; $n = 3$; $^*p < 0.05$, $^{***}p = 0.001$, paired-samples *t* test).

higher than in the control (*pcDNA6.2–EmGFP* "empty" vector)-transfected cells (Fig. 8*E*,*F*). This is most likely attributable to the repression of the sensor vectors by the endogenous expression of *miR-200c* in COS-7 cells (data not shown). Our results show that *miR-200c* regulates the expression levels of Sox2 and E2F3 by directly binding to conserved BS(s) within the 3′UTR of their mRNAs.

Sox2 and E2F3 directly activate the *mmu-miR-200c/141* promoter

Although Sox2 and E2F3 are direct targets of *miR-200c*, both TFs are coexpressed with *miR-200c* in at least a subpopulation of vMH neural progenitors (Figs. 4*D*, 5*A*). We therefore hypothesized that Sox2 and E2F3 might in turn regulate the expression of the *miR-200* family in neural progenitor cells. To test this hypothesis, we first searched for conserved Sox2 and E2F BSs within the *miR-200c/141* promoter region (−2 kb to +500 bp) using the Gene2promoter software (Genomatix). We then cloned the distal (*Promoter 1*) and proximal (*Promoter 2*) promoter region of the *mmu-miR-200c/141* cluster harboring several conserved Sox2 (sequence: AACAAAG) and/or E2F (core sequence: GCGC) BSs into a luciferase reporter vector (Fig. 9*A*). Cotransfection of this *pGL3–mmu-miR-200c/141* reporter vector together with vectors encoding Sox2 or E2F3 into HEK-293 cells led to a 3- and 3.4-fold activation of the distal *mmu-miR-200c/141* promoter region (*Promoter 1* containing conserved Sox2 and E2F BSs) by E2F3 and Sox2, respectively, and to a fivefold activation of the proximal *mmu-miR-200c/141* promoter region (*Promoter 2* containing only conserved E2F BSs) by E2F3 (Fig. 9*B*). These data indicate that the transcription of the *mmu-miR-200c/141* gene cluster is in fact activated by Sox2 and to an even greater extent by E2F3 TFs. Altogether, our data

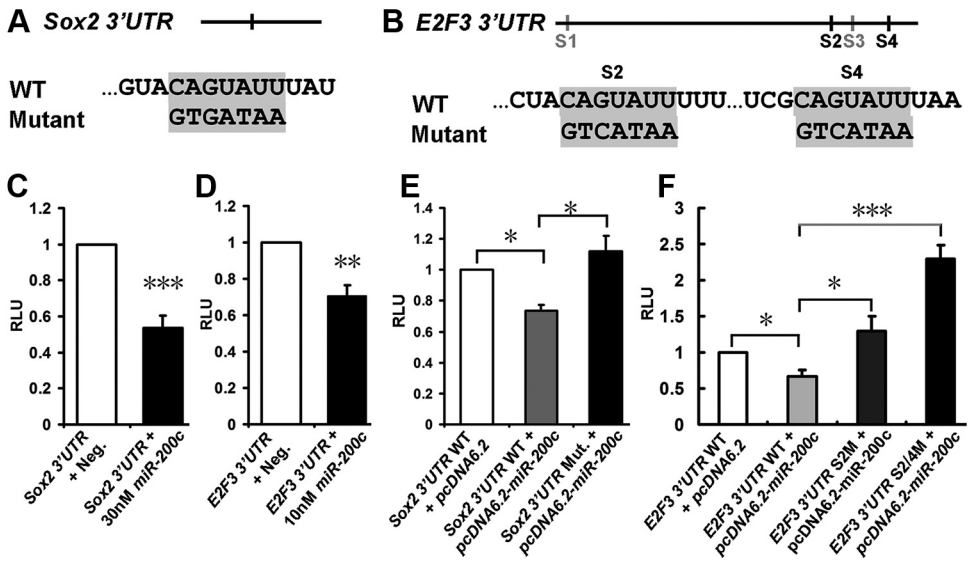

Figure 8. *miR-200c* targets directly the *Sox2* and *E2F3* 3′UTRs. ***A***, Top, Relative position of the conserved *miR-200c/b/429* BS within the mouse *Sox2* 3′UTR. Bottom, Sequence of the wild-type (WT) and mutated (mutant) *miR-200c/b/429* BS in the mouse *Sox2* 3′UTR. Seed regions/sequences are highlighted in gray. ***B***, Top, Relative positions of four conserved (in mammals) BSs for the *miR-200* family within the mouse *E2F3* 3′UTR. BS1 and BS3 (S1 and S3, gray bars) are complementary to the *miR-200a/141* seed sequence, and BS2 and BS4 (S2 and S4, black bars) are complementary to the *miR-200c/b/429* seed sequence. The *E2F3* 3′UTR containing S2–S4 was used for the sensor assays. Bottom, Sequence of the wild-type (WT) and mutated (mutant) *miR-200c/b/429* BSs (S2 and S4) in the mouse *E2F3* 3′UTR. Seed regions/sequences are highlighted in gray. ***C***, ***D***, Transfection of 30 nM (*Sox2*) or 10 nM (*E2F3*) *mmu-miR-200c* precursor miRNA in COS-7 cells repressed the luciferase expression from the *pGL3–Sox2–3′UTR* and *pGL3–E2F3–3′UTR* sensor vectors compared with cells transfected with a negative control (Neg.) precursor miRNA (negative control value was set as 1; 30 nM *mmu-miR-200c* precursor + *Sox2* 3′UTR: 0.538 ± 0.068; 10 nM *mmu-miR-200c* precursor + *E2F3* 3′UTR: 0.705 ± 0.061; $n = 3$; ***$p < 0.005$, **$p < 0.01$, independent-samples *t* test). ***E***, Overexpression of *miR-200c* (using the *pcDNA6.2–EmGFP–miR-200c* vector) in COS-7 cells led to a downregulation of luciferase expression from the *pGL3–Sox2–3′UTR* sensor vector containing the wild-type (WT) *Sox2* 3′UTR, which was rescued after site-directed mutagenesis of the *miR-200c* seed sequence within the *Sox2* 3′UTR (Mut.). Transfection of the sensor vector together with "empty" *pcDNA6.2–EmGFP* vector served as negative control, and this value was set as 1. (*Sox2* 3′UTR WT + *pcDNA6.2–miR-200c*: 0.737 ± 0.037; *Sox2* 3′UTR Mut. + *pcDNA6.2–miR-200c*: 1.12 ± 0.1; $n = 3$; *$p < 0.05$, independent-samples *t* test). ***F***, Overexpression of *miR-200c* (using the *pcDNA6.2–EmGFP–miR-200c* vector) in COS-7 cells led to a downregulation of luciferase expression from the *pGL3–E2F3–3′UTR* sensor vector containing the wild-type (WT) *E2F3* 3′UTR, which was rescued after site-directed mutagenesis of the two *miR-200c* seed sequences within the *E2F3* 3′UTR (S2M and S2/4M). Transfection of the sensor vector together with "empty" *pcDNA6.2–EmGFP* vector served as negative control, and this value was set as 1. (*E2F3* 3′UTR WT + *pcDNA6.2–miR-200c*: 0.667 ± 0.09; *E2F3* 3′UTR S2M + *pcDNA6.2–miR-200c*: 1.3 ± 0.2; *E2F3* 3′UTR S2/4M + *pcDNA6.2–miR-200c*: 2.29 ± 0.19; $n = 3$; *$p < 0.05$, ***$p < 0.005$ in the independent-samples *t* test.) RLU, Relative luciferase units.

strongly suggest that the *miR-200* family is engaged in an unilateral negative feedback loop with Sox2 and E2F3 ensuring the proper regulation of Sox2 and E2F3 mRNA and/or protein levels in vMH neural progenitor cells (Fig. 9*C*), thereby facilitating their cell-cycle exit and differentiation into postmitotic neurons.

Discussion

We show here that the depletion of Dicer1-processed mature miRNAs and in particular of *miR-200* in the MHR of the *Dicer1 cKO* embryos leads to the progressive loss of this region because of a strong increase of apoptotic cell death in the dorsal MHR and the failure of vMH neural progenitors to exit the cell cycle and to generate the appropriate numbers of neuronal offspring. We propose that the *miR-200* family belongs to a novel class of miRNAs that are engaged in an unilateral negative feedback loop with their direct targets Sox2 and E2F3 (Fig. 9*D*), thereby promoting the transition from a proliferating and pluripotent/multipotent to a postmitotic and differentiating neural cell in the murine CNS.

Dicer1-processed miRNAs are not required for the patterning of the murine MHR

Although the progressive loss of the MHR in the *Dicer1 cKO* embryos resulted in a morphological defect at birth that strongly resembled the phenotype of mouse mutants for some of the IsO genes (Wurst and Bally-Cuif, 2001; Zervas et al., 2005), the MHR was correctly patterned along its A/P and D/V axes in the *Dicer1 cKO* embryos. We concluded that the morphological defects of the *Dicer1 cKO* embryos are not attributable to a deregulation of IsO gene expression in the absence of Dicer1-processed miRNAs, including *miR-200* and *miR-124*, one of the most abundant miRNAs in the brain (Lagos-Quintana et al., 2002). Similar observations were made in another conditional *Dicer1* mutant [*Wnt1–Cre*; *Dicer1*$^{flox/flox}$ mice (Huang et al., 2010)] and in other organs/tissues after *Dicer1* deletion (Harfe et al., 2005; Choi et al., 2008; Kawase-Koga et al., 2010), thus corroborating the assumption that Dicer1-processed miRNAs do not play a major role in early patterning events during mouse embryogenesis.

Dicer1-processed miRNAs are necessary for the proper survival of neural cells in the murine MHR

The massive increase of apoptotic cell death in the *Dicer1 cKO* embryos from E11.5 onward most likely caused the progressive dorsal MH tissue loss in these embryos. Increased apoptosis is a unifying feature of almost all conditional *Dicer1* mutants, particularly in the nervous system (Coolen and Bally-Cuif, 2009). Pro-apoptotic proteins were relatively enriched, whereas pro-survival proteins were depleted in *Dicer1*-deficient neural stem cells (NSCs) (Kawase-Koga et al., 2010), and it is therefore very likely that proapoptotic and/or prosurvival pathways are also deregulated in the MHR of our *Dicer1 cKO* mice. However, the far lesser amount of apoptotic cell death in the mutant ventral MHR, especially at midgestational stages, cannot explain the drastic reduction of mDA, RN, and 5-HT but not of OM neurons observed already at these early stages after depletion of Dicer1-processed mature miRNAs in the *Dicer1 cKO* embryos.

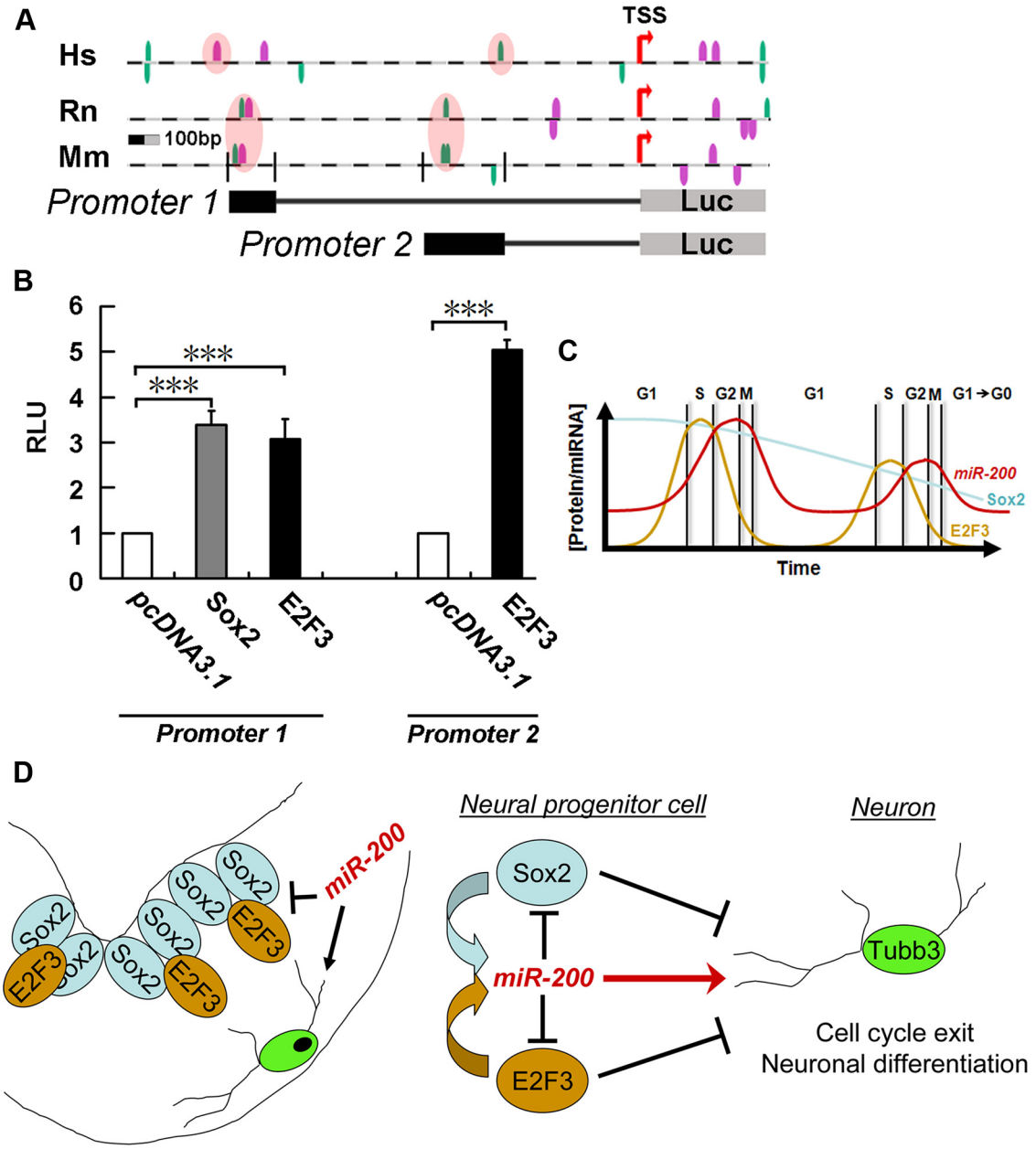

Figure 9. The *mmu-miR-200c/141* promoter is activated by Sox2 and E2F3. ***A***, Position and sequence of conserved (highlighted by pink ovals) BSs for Sox2 (magenta) and E2F (green) TFs within the human (Hs), rat (Rn), and mouse (Mm) *miR-200c/141* distal (Promoter 1) and proximal (Promoter 2) promoter regions. The mouse *mmu-miR-200c/141* promoter regions (black boxes) were cloned in front of the Luciferase (Luc) CDS to obtain the corresponding reporter vectors. TSS, Transcription start site. ***B***, Strong activation of the distal (Promoter 1) *mmu-miR-200c/141* promoter region was seen after cotransfection of the reporter vector and *Sox2* or *E2F3* cDNA in HEK-293 cells. An even stronger activation of the proximal (Promoter 2) *mmu-miR-200c/141* promoter region was detected after cotransfection of the reporter vector and *E2F3* cDNA. Cotransfection of the reporter vectors and *pcDNA3.1* ("empty") vector was used as negative control, and this value was set as 1. [*pGL3–mmu-miR-200c/141* (Promoter 1) + Sox2: 3.38 ± 0.31; *pGL3–mmu-miR-200c/141* (Promoter 1) + E2F3: 3.08 ± 0.44; *pGL3–mmu-miR-200c/141* (Promoter 2) + E2F3: 5.03 ± 0.23; $n = 4$; ***$p < 0.001$, independent-samples *t* test). RLU, Relative luciferase units. ***C***, The cyclic expression of E2F3 protein and presumably stronger regulatory interaction between E2F3 and *miR-200* (more E2F3/*miR-200* BSs within the *miR-200c/141* promoter/*E2F3* 3′UTR, respectively, compared with Sox2) are predicted to result in an oscillatory expression of E2F3/*miR-200* and gradual reduction of Sox2 (blue)/E2F3 (brown) protein and *miR-200* (red) miRNA levels in neural stem/progenitor cells, thereby promoting their cell-cycle exit and neuronal differentiation. Note that we do not provide any evidence for an oscillatory expression of *miR-200* family members in neural stem/progenitor cells. G1, S, G2, M, G0, Phases of the cell cycle. ***D***, Proposed model for the unilateral negative feedback loop between Sox2/E2F3-mediated activation of *miR-200* (red) transcription and, in turn, *miR-200*-mediated translational inhibition of Sox2 (blue circles)/E2F3 (brown circles) expression in neural stem/progenitor cells located within the VZ/SVZ and IZ of the murine MHR. Note that these two TFs and *miR-200c* are coexpressed in neural stem/progenitor cells. The unilateral negative feedback loop between *miR-200* and Sox2/E2F3 promotes the cell-cycle exit and neuronal differentiation of vMH neural progenitors.

MiR-200 family miRNAs promote the cell-cycle exit and neuronal differentiation of vMH neural progenitors

Another reason for the strong reduction of selected vMH neuronal populations in the *Dicer1 cKO* embryos was the failure of the corresponding neural progenitors to exit the cell cycle and to generate the appropriate amount of postmitotic neurons. This finding might also explain the relative sparing of the OM neurons in the mutant embryos: OM neurons are among the earliest-born neurons in the murine ventral midbrain [approximately E9.5 (Prakash et al., 2009)] and might thus have become postmitotic by their majority before the depletion of Dicer1-processed miRNAs in the *Dicer1 cKO* embryos affected their progenitors. In support of

our findings, *Dicer1*-deficient cortical NSCs also fail to generate the appropriate amount of neuronal and glial progeny and undergo premature apoptosis in the absence of growth-promoting factors, although obvious cell-cycle defects were not detected in these cases (De Pietri Tonelli et al., 2008; Andersson et al., 2010; Kawase-Koga et al., 2010).

miRNAs are widely implicated in the cell-cycle control of pluripotent/multipotent stem/progenitor cells and in their differentiation into a committed cell fate (Wang and Blelloch, 2009; Ivey and Srivastava, 2010; Mallanna and Rizzino, 2010). However, miRNAs can persist in neural stem/progenitor cells at relatively high levels and over a considerable time after *Dicer1* inactivation (Andersson et al., 2010). In search for the most strongly depleted miRNA(s) in the MHR of the *Dicer1 cKO* embryos, we identified the entire *miR-200* family as possible candidates that might cause the cell-cycle exit/differentiation defects in the mutants. *miR-200c*, a member of this family, is highly expressed in neural stem/progenitor cells of the MHR and other regions of the brain (data not shown), suggesting a function of this miRNA family in multipotent neural stem/progenitor cells. In fact, overexpression of *miR-200* family members promoted, whereas the knockdown of this family in primary vMH cultures or their loss in the *Dicer1 cKO* embryos inhibited, the cell-cycle exit and neuronal differentiation of proliferating vMH neural progenitors. It appears that this function of the *miR-200* family is highly context dependent: in some cases, these miRNAs promote (Brabletz and Brabletz, 2010), whereas in other cases they rather inhibit, the differentiation of pluripotent or dedifferentiated stem cells (Lin et al., 2009; Gill et al., 2011).

miR-200 and their targets Sox2 and E2F3 are engaged in a unilateral negative feedback loop to direct cell-cycle exit and differentiation of neural progenitors

We found that the *miR-200* family (in particular *miR-200c*) promotes cell-cycle exit and neuronal differentiation of vMH neural progenitors by downregulating Sox2 and E2F3 expression in these cells and that *miR-200c* directly targets the *Sox2* and *E2F3* mRNAs via specific BSs in their 3′UTRs. Sox2 is required in a dose-dependent manner for maintaining the multipotency of neural stem/progenitor cells and inhibiting their cell-cycle exit and differentiation into neurons or glial cells (Avilion et al., 2003; Graham et al., 2003; Pevny and Nicolis, 2010). E2F3 protein levels/activity accumulate cyclically during the late G_1-phase of the cell cycle, thereby promoting the transition from G_1 to S-phase in proliferating cells by activating genes involved in DNA replication and cell-cycle regulation (Leone et al., 1998; Humbert et al., 2000; Chong et al., 2009). Several of the E2F3-regulated genes also belong to proapoptotic/antiapoptotic, intracellular signaling, and other pathways implicated in cell survival and differentiation (Müller et al., 2001; DeGregori, 2002). Because the complete loss of activating E2F TFs (E2F1–E2F3) *in vivo* does not affect the proliferation of multipotent stem/progenitor cells but decreases their survival (Chong et al., 2009), *miR-200* might additionally promote the survival of vMH neural progenitors by regulating E2F3 protein levels in these cells.

We also found that Sox2 and E2F3 directly activate the distal and proximal promoter regions of the murine *miR-200c/141* gene cluster, in agreement with the coexpression of these two TFs and *miR-200c* in neural progenitors. This unilateral negative feedback loop of Sox2/E2F3 and *miR-200c/141* is predicted to result in an oscillatory expression of E2F3/*miR-200* in neural progenitors (Krol et al., 2010): initially high levels of Sox2 and increasing levels of E2F3 protein activate *miR-200c/141* expression, which in turn lower Sox2/E2F3 protein levels in these cells, leading to the downregulation of *miR-200c/141* and the (re-)activation of Sox2/E2F3 expression (Fig. 9*C*). This oscillatory regulation might thus contribute to the cyclic accumulation of E2F3 protein/transcriptional activity only during the late G_1-phase of the cell cycle, despite the continuous expression of *E2F3* mRNA in proliferating cells (Leone et al., 1998). In fact, E2F3 protein was accumulating aberrantly in *Dicer1*-mutant S-phase neural progenitors. In addition, the *miR-200*-mediated negative regulation of the autoactivating Sox2 and E2F3 TFs (Adams et al., 2000; Tomioka et al., 2002) might result in a gradual reduction of Sox2 and E2F3 protein levels and eventually lead to the complete silencing [below a certain threshold (Mukherji et al., 2011)] of these two and other pluripotency/multipotency and cell-cycle regulatory genes in neural progenitors (Fig. 9*C*). Our findings are also supported by data showing that the pluripotency factor Lin28 binds to the *pre-miR-200c* stem loop and targets it for degradation, thereby inhibiting its processing into mature *miR-200c* in undifferentiated cells (Heo et al., 2009). The *miR-200* family might thus only become active when the neural progenitor cells transit to a more committed cell fate by downregulating the expression of pluripotency factors such as Lin28.

Altogether, our results strongly support the notion that the *miR-200* family members cooperate to suppress the levels of Sox2 and E2F3 proteins below a critical level, thereby enabling the cell-cycle exit of neural progenitors and subsequently their differentiation into neurons (Fig. 9*D*), although we cannot exclude that the two *miR-200* seed sequence subgroups might slightly differ in their target genes (Uhlmann et al., 2010) and that the two *miR-200* gene clusters might be regulated by a distinct set of transcriptional activators/repressors. We have studied the mutual regulation of Sox2/E2F3 and *miR-200* using *in vitro* paradigms that might not reflect entirely the *in vivo* situation. The relatively subtle effects observed after *miR-200* overexpression/knockdown in cultured vMH cells indicate that, because of the early and widespread functions of the *miR-200* family (Peter, 2009; Brabletz and Brabletz, 2010) as well as the early and redundant functions of the SoxB1 (including Sox2) (Pevny and Nicolis, 2010) and E2F (DeGregori, 2002) TFs during murine development, the generation of conditional mouse mutants for the two *miR-200* gene clusters comprising all five *miR-200* family members and for the SoxB1/E2F TFs expressed in neural stem/progenitor cells will be required to ultimately establish the function of the regulatory interaction of *miR-200* and Sox2/E2F3 in these cells *in vivo*. Nevertheless, this miRNA family might represent an intermediate (third) functional group of miRNAs in the mammalian CNS, allocated between the ESCC miRNAs ensuring the pluripotent state of NSCs and neuron-specific miRNAs supporting the proper differentiation of these cells into neurons (Coolen and Bally-Cuif, 2009; Mallanna and Rizzino, 2010).

References

Adams MR, Sears R, Nuckolls F, Leone G, Nevins JR (2000) Complex transcriptional regulatory mechanisms control expression of the E2F3 locus. Mol Cell Biol 20:3633–3639. CrossRef Medline

Ameres SL, Horwich MD, Hung JH, Xu J, Ghildiyal M, Weng Z, Zamore PD (2010) Target RNA-directed trimming and tailing of small silencing RNAs. Science 328:1534–1539. CrossRef Medline

Andersson T, Rahman S, Sansom SN, Alsiö JM, Kaneda M, Smith J, O'Carroll D, Tarakhovsky A, Livesey FJ (2010) Reversible block of mouse neural stem cell differentiation in the absence of dicer and microRNAs. PLoS One 5:e13453. CrossRef Medline

Avilion AA, Nicolis SK, Pevny LH, Perez L, Vivian N, Lovell-Badge R (2003) Multipotent cell lineages in early mouse development depend on SOX2 function. Genes Dev 17:126–140. CrossRef Medline

Bibel M, Richter J, Lacroix E, Barde YA (2007) Generation of a defined and uniform population of CNS progenitors and neurons from mouse embryonic stem cells. Nat Protoc 2:1034–1043. CrossRef Medline

Brabletz S, Brabletz T (2010) The ZEB/miR-200 feedback loop—a motor of cellular plasticity in development and cancer? EMBO Rep 11:670–677. CrossRef Medline

Chi CL, Martinez S, Wurst W, Martin GR (2003) The isthmic organizer signal FGF8 is required for cell survival in the prospective midbrain and cerebellum. Development 130:2633–2644. CrossRef Medline

Choi PS, Zakhary L, Choi WY, Caron S, Alvarez-Saavedra E, Miska EA, McManus M, Harfe B, Giraldez AJ, Horvitz HR, Schier AF, Dulac C (2008) Members of the miRNA-200 family regulate olfactory neurogenesis. Neuron 57:41–55. CrossRef Medline

Chong JL, Wenzel PL, Sáenz-Robles MT, Nair V, Ferrey A, Hagan JP, Gomez YM, Sharma N, Chen HZ, Ouseph M, Wang SH, Trikha P, Culp B, Mezache L, Winton DJ, Sansom OJ, Chen D, Bremner R, Cantalupo PG, Robinson ML, Pipas JM, Leone G (2009) E2f1–3 switch from activators in progenitor cells to repressors in differentiating cells. Nature 462:930–934. CrossRef Medline

Cobb BS, Nesterova TB, Thompson E, Hertweck A, O'Connor E, Godwin J, Wilson CB, Brockdorff N, Fisher AG, Smale ST, Merkenschlager M (2005) T cell lineage choice and differentiation in the absence of the RNase III enzyme Dicer. J Exp Med 201:1367–1373. CrossRef Medline

Coolen M, Bally-Cuif L (2009) MicroRNAs in brain development and physiology. Curr Opin Neurobiol 19:461–470. CrossRef Medline

De Pietri Tonelli D, Pulvers JN, Haffner C, Murchison EP, Hannon GJ, Huttner WB (2008) miRNAs are essential for survival and differentiation of newborn neurons but not for expansion of neural progenitors during early neurogenesis in the mouse embryonic neocortex. Development 135:3911–3921. CrossRef Medline

DeGregori J (2002) The genetics of the E2F family of transcription factors: shared functions and unique roles. Biochim Biophys Acta 1602:131–150. Medline

Ebert MS, Neilson JR, Sharp PA (2007) MicroRNA sponges: competitive inhibitors of small RNAs in mammalian cells. Nat Methods 4:721–726. CrossRef Medline

Fischer T, Guimera J, Wurst W, Prakash N (2007) Distinct but redundant expression of the Frizzled Wnt receptor genes at signaling centers of the developing mouse brain. Neuroscience 147:693–711. CrossRef Medline

Fischer T, Faus-Kessler T, Welzl G, Simeone A, Wurst W, Prakash N (2011) Fgf15-mediated control of neurogenic and proneural gene expression regulates dorsal midbrain neurogenesis. Dev Biol 350:496–510. CrossRef Medline

Gill JG, Langer EM, Lindsley RC, Cai M, Murphy TL, Kyba M, Murphy KM (2011) Snail and the microRNA-200 family act in opposition to regulate epithelial-to-mesenchymal transition and germ layer fate restriction in differentiating ESCs. Stem Cells 29:764–776. CrossRef Medline

Graham V, Khudyakov J, Ellis P, Pevny L (2003) SOX2 functions to maintain neural progenitor identity. Neuron 39:749–765. CrossRef Medline

Guillemot F, Zimmer C (2011) From cradle to grave: the multiple roles of fibroblast growth factors in neural development. Neuron 71:574–588. CrossRef Medline

Guo C, Qiu HY, Huang Y, Chen H, Yang RQ, Chen SD, Johnson RL, Chen ZF, Ding YQ (2007) Lmx1b is essential for Fgf8 and Wnt1 expression in the isthmic organizer during tectum and cerebellum development in mice. Development 134:317–325. CrossRef Medline

Harfe BD, McManus MT, Mansfield JH, Hornstein E, Tabin CJ (2005) The RNaseIII enzyme Dicer is required for morphogenesis but not patterning of the vertebrate limb. Proc Natl Acad Sci U S A 102:10898–10903. CrossRef Medline

Heo I, Joo C, Kim YK, Ha M, Yoon MJ, Cho J, Yeom KH, Han J, Kim VN (2009) TUT4 in concert with Lin28 suppresses microRNA biogenesis through pre-microRNA uridylation. Cell 138:696–708. CrossRef Medline

Hirata H, Tomita K, Bessho Y, Kageyama R (2001) Hes1 and Hes3 regulate maintenance of the isthmic organizer and development of the mid/hindbrain. EMBO J 20:4454–4466. CrossRef Medline

Huang T, Liu Y, Huang M, Zhao X, Cheng L (2010) Wnt1-cre-mediated conditional loss of Dicer results in malformation of the midbrain and cerebellum and failure of neural crest and dopaminergic differentiation in mice. J Mol Cell Biol 2:152–163. CrossRef Medline

Humbert PO, Verona R, Trimarchi JM, Rogers C, Dandapani S, Lees JA (2000) E2f3 is critical for normal cellular proliferation. Genes Dev 14:690–703. Medline

Huntzinger E, Izaurralde E (2011) Gene silencing by microRNAs: contributions of translational repression and mRNA decay. Nat Rev Genet 12:99–110. CrossRef Medline

Ivey KN, Srivastava D (2010) MicroRNAs as regulators of differentiation and cell fate decisions. Cell Stem Cell 7:36–41. CrossRef Medline

Kawase-Koga Y, Low R, Otaegi G, Pollock A, Deng H, Eisenhaber F, Maurer-Stroh S, Sun T (2010) RNAase-III enzyme Dicer maintains signaling pathways for differentiation and survival in mouse cortical neural stem cells. J Cell Sci 123:586–594. CrossRef Medline

Kimmel RA, Turnbull DH, Blanquet V, Wurst W, Loomis CA, Joyner AL (2000) Two lineage boundaries coordinate vertebrate apical ectodermal ridge formation. Genes Dev 14:1377–1389. Medline

Kozomara A, Griffiths-Jones S (2011) miRBase: integrating microRNA annotation and deep-sequencing data. Nucleic Acids Res 39:D152–D157. CrossRef Medline

Krichevsky AM, Sonntag KC, Isacson O, Kosik KS (2006) Specific microRNAs modulate embryonic stem cell-derived neurogenesis. Stem Cells 24:857–864. CrossRef Medline

Krol J, Loedige I, Filipowicz W (2010) The widespread regulation of microRNA biogenesis, function and decay. Nat Rev Genet 11:597–610. CrossRef Medline

Lagos-Quintana M, Rauhut R, Yalcin A, Meyer J, Lendeckel W, Tuschl T (2002) Identification of tissue-specific microRNAs from mouse. Curr Biol 12:735–739. CrossRef Medline

Lau P, Verrier JD, Nielsen JA, Johnson KR, Notterpek L, Hudson LD (2008) Identification of dynamically regulated microRNA and mRNA networks in developing oligodendrocytes. J Neurosci 28:11720–11730. CrossRef Medline

Leone G, DeGregori J, Yan Z, Jakoi L, Ishida S, Williams RS, Nevins JR (1998) E2F3 activity is regulated during the cell cycle and is required for the induction of S phase. Genes Dev 12:2120–2130. CrossRef Medline

Li R, Li Y, Kristiansen K, Wang J (2008) SOAP: short oligonucleotide alignment program. Bioinformatics 24:713–714. CrossRef Medline

Lin CH, Jackson AL, Guo J, Linsley PS, Eisenman RN (2009) Myc-regulated microRNAs attenuate embryonic stem cell differentiation. EMBO J 28:3157–3170. CrossRef Medline

Livak KJ, Schmittgen TD (2001) Analysis of relative gene expression data using real-time quantitative PCR and the 2(-Delta Delta C(T)) method. Methods 25:402–408. CrossRef Medline

Mallanna SK, Rizzino A (2010) Emerging roles of microRNAs in the control of embryonic stem cells and the generation of induced pluripotent stem cells. Dev Biol 344:16–25. CrossRef Medline

Martinez NJ, Gregory RI (2010) MicroRNA gene regulatory pathways in the establishment and maintenance of ESC identity. Cell Stem Cell 7:31–35. CrossRef Medline

McMahon AP, Bradley A (1990) The Wnt-1 (int-1) proto-oncogene is required for development of a large region of the mouse brain. Cell 62:1073–1085. CrossRef Medline

Mukherji S, Ebert MS, Zheng GX, Tsang JS, Sharp PA, van Oudenaarden A (2011) MicroRNAs can generate thresholds in target gene expression. Nat Genet 43:854–859. CrossRef Medline

Müller H, Bracken AP, Vernell R, Moroni MC, Christians F, Grassilli E, Prosperini E, Vigo E, Oliner JD, Helin K (2001) E2Fs regulate the expression of genes involved in differentiation, development, proliferation, and apoptosis. Genes Dev 15:267–285. CrossRef Medline

Nakamura T, Colbert MC, Robbins J (2006) Neural crest cells retain multipotential characteristics in the developing valves and label the cardiac conduction system. Circ Res 98:1547–1554. CrossRef Medline

Pauli A, Rinn JL, Schier AF (2011) Non-coding RNAs as regulators of embryogenesis. Nat Rev Genet 12:136–149. CrossRef Medline

Peng C, Fan S, Li X, Fan X, Ming M, Sun Z, Le W (2007) Overexpression of Pitx3 upregulates expression of BDNF and GDNF in SH-SY5Y cells and primary ventral mesencephalic cultures. FEBS Lett 581:1357–1361. CrossRef Medline

Peng C, Aron L, Klein R, Li M, Wurst W, Prakash N, Le W (2011) Pitx3 is a critical mediator of GDNF-induced BDNF expression in nigrostriatal dopaminergic neurons. J Neurosci 31:12802–12815. CrossRef Medline

Peter ME (2009) Let-7 and miR-200 microRNAs: guardians against pluripotency and cancer progression. Cell Cycle 8:843–852. CrossRef Medline

Pettitt SJ, Liang Q, Rairdan XY, Moran JL, Prosser HM, Beier DR, Lloyd KC,

Bradley A, Skarnes WC (2009) Agouti C57BL/6N embryonic stem cells for mouse genetic resources. Nat Methods 6:493–495. CrossRef Medline

Pevny LH, Nicolis SK (2010) Sox2 roles in neural stem cells. Int J Biochem Cell Biol 42:421–424. CrossRef Medline

Prakash N, Puelles E, Freude K, Trümbach D, Omodei D, Di Salvio M, Sussel L, Ericson J, Sander M, Simeone A, Wurst W (2009) Nkx6–1 controls the identity and fate of red nucleus and oculomotor neurons in the mouse midbrain. Development 136:2545–2555. CrossRef Medline

Puelles E, Annino A, Tuorto F, Usiello A, Acampora D, Czerny T, Brodski C, Ang SL, Wurst W, Simeone A (2004) Otx2 regulates the extent, identity and fate of neuronal progenitor domains in the ventral midbrain. Development 131:2037–2048. CrossRef Medline

Rubinson DA, Dillon CP, Kwiatkowski AV, Sievers C, Yang L, Kopinja J, Rooney DL, Zhang M, Ihrig MM, McManus MT, Gertler FB, Scott ML, Van Parijs L (2003) A lentivirus-based system to functionally silence genes in primary mammalian cells, stem cells and transgenic mice by RNA interference. Nat Genet 33:401–406. CrossRef Medline

Schwarz M, Alvarez-Bolado G, Urbánek P, Busslinger M, Gruss P (1997) Conserved biological function between Pax-2 and Pax-5 in midbrain and cerebellum development: evidence from targeted mutations. Proc Natl Acad Sci U S A 94:14518–14523. CrossRef Medline

Silahtaroglu AN, Nolting D, Dyrskjøt L, Berezikov E, Møller M, Tommerup N, Kauppinen S (2007) Detection of microRNAs in frozen tissue sections by fluorescence in situ hybridization using locked nucleic acid probes and tyramide signal amplification. Nat Protoc 2:2520–2528. CrossRef Medline

Simon HH, Saueressig H, Wurst W, Goulding MD, O'Leary DD (2001) Fate of midbrain dopaminergic neurons controlled by the engrailed genes. J Neurosci 21:3126–3134. Medline

Tomioka M, Nishimoto M, Miyagi S, Katayanagi T, Fukui N, Niwa H, Muramatsu M, Okuda A (2002) Identification of Sox-2 regulatory region which is under the control of Oct-3/4-Sox-2 complex. Nucleic Acids Res 30:3202–3213. CrossRef Medline

Uhlmann S, Zhang JD, Schwäger A, Mannsperger H, Riazalhosseini Y, Burmester S, Ward A, Korf U, Wiemann S, Sahin O (2010) miR-200bc/429 cluster targets PLCgamma1 and differentially regulates proliferation and EGF-driven invasion than miR-200a/141 in breast cancer. Oncogene 29:4297–4306. CrossRef Medline

Wang Y, Blelloch R (2009) Cell cycle regulation by MicroRNAs in embryonic stem cells. Cancer Res 69:4093–4096. CrossRef Medline

Wang Y, Baskerville S, Shenoy A, Babiarz JE, Baehner L, Blelloch R (2008) Embryonic stem cell-specific microRNAs regulate the G1-S transition and promote rapid proliferation. Nat Genet 40:1478–1483. CrossRef Medline

Wittmann DM, Blöchl F, Trümbach D, Wurst W, Prakash N, Theis FJ (2009) Spatial analysis of expression patterns predicts genetic interactions at the mid-hindbrain boundary. PLoS Comput Biol 5:e1000569. CrossRef Medline

Wurst W, Bally-Cuif L (2001) Neural plate patterning: upstream and downstream of the isthmic organizer. Nat Rev Neurosci 2:99–108. CrossRef Medline

Wurst W, Auerbach AB, Joyner AL (1994) Multiple developmental defects in Engrailed-1 mutant mice: an early mid-hindbrain deletion and patterning defects in forelimbs and sternum. Development 120:2065–2075. Medline

Zervas M, Blaess S, Joyner AL (2005) Classical embryological studies and modern genetic analysis of midbrain and cerebellum development. Curr Top Dev Biol 69:101–138. CrossRef Medline